The Health Benefits of Solar Power Generation: Evidence from Chile

Nathaly M. Rivera*†

Elisheba Spiller‡

J. Cristobal Ruiz-Tagle§

Abstract

Renewable energy can yield social benefits through local air quality improvements and their subsequent effects on human health. We estimate some of these benefits using data gathered during the rapid adoption of large-scale solar power generation in Chile over the last decade. Relying on exogenous variation from incremental solar generation capacity over time, we find that solar energy displaces fossil fuel generation (primarily coal-fired generation) and curtails hospital admissions, particularly those due to lower respiratory diseases. These effects are noted mostly in cities downwind of displaced fossil fuel generation and are present across all age groups. Our results document the existence of an additional channel through which renewable energy can increase social welfare.

Keywords: Coal-fired power plants, coal displacement, solar generation, power plants, pollution, morbidity, developing countries, Latin America
JEL classification numbers: I18, L94, Q42, Q53

*We thank Andrew Bibler, Janet Currie, Harrison Fell, Maria Harris, Sarah Jacobson, Nicolai Kuminoff, Lucija Muehlenbachs, Subhrendu K. Pattanayak, and Brett Watson for helpful comments and suggestions. We also thank seminar participants at the Environmental Defense Fund, Grantham Workshop, Manhatan College, Universidad Adolfo Ibañez, Universidad Católica del Norte, University of São Paulo, University of Talca, and workshop and conference participants at the 21st Annual CU Environmental and Resource Economics Workshop, the 25th Annual Conference of the European Association of Environmental and Resource Economists, the Association of Environmental and Resource Economists Annual Summer Conference, Camp Resources XXVI, the 7th Canadian Resource and Environmental Economics Association Workshop, the Eastern Economic Association Annual Meeting 2020, the Empirical Methods in Energy Economics Summer Workshop 2021, SETI Annual Meetings, Tercer Workshop sobre Economía del Medio Ambiente y Cambio Climático, and the Western Economic Association International Annual Conference 2021, for helpful comments and suggestions. All errors are ours.

†University of São Paulo, ✉: nmrivera@usp.br.

‡Environmental Defense Fund, ✉: espiller@edf.org.

§London School of Economics and Political Science, ✉: cristobal.ruiztagle@gmail.com.

1 Introduction

Renewable energy is the world's fastest-growing energy source, set to become the leading source of primary energy consumption by 2050 (U.S. Energy Information Administration, 2019). It promises several benefits to society, ranging from reductions in greenhouse gas emissions, lower discharge of local air pollutants, and improved health outcomes, to reduced dependence on imported fuels and the creation of jobs through the manufacturing and installation of these resources (U.S. Environmental Protection Agency, 2019). Yet we still lack a good understanding of the magnitude of some of these benefits, notably those associated with reduced air pollution and health improvements. In this work, we use the rapid adoption of large-scale solar power generation in the desert region of northern Chile to empirically quantify some of the health benefits of solar energy through improvements in air quality.

Fossil fuel power generation, particularly that from coal combustion, releases large amounts of local air pollutants, including sulfur dioxide (SO_2), nitrogen oxides (NO_X), and particulate matter (PM). These pollutants are associated with several adverse health effects, along with increased hospital admissions, mortality risks, and threats to life expectancy.[1] The extent to which these emissions are curtailed with the introduction of renewables reflects the potential of alternative energy sources to offset some of the negative effects of dirty electricity generation. Nonetheless, some fossil fuel plants (e.g., natural gas plants) have consistently been dispatched to deal with the intermittency of renewables (Fell and Linn, 2013), thus attenuating the benefits of increasing the supply of these sources. More insights on the co-benefits of renewable energy are, therefore, crucial to the cost-benefit analyses of transitioning away from fossil fuels and, thus, for the optimal design of energy policy.

The Atacama Desert, one of the sunniest and driest deserts in the world, not only has the highest average surface solar radiation worldwide (Rondanelli et al., 2015), but also the highest solar power potential. Figure 1 shows Chile's photovoltaic power potential—a solar energy system's maximum productivity over time—relative to the rest of the world. This potential, together with the recent decline in the cost of photovoltaic (PV) technology and the country's regulations aimed at fostering the adoption of renewables, resulted in rapid market penetration of solar generation in Chile. By the end of 2012, a variety of solar plants with capacity ranging from 3 MW to 138 MW were already injecting electricity into Chile's northern electric grid, and by 2017, solar generators were producing about 10 percent of total electricity in Chile's northern grid. We take advantage of this surge in large-scale investments in solar energy to explore the effects of the steady expansion in solar capacity

[1] For comprehensive reviews, see Currie et al. (2014) on the effects of early-life exposure to pollution, and Hoek et al. (2013) on the mortality impact of long-term air pollution exposure.

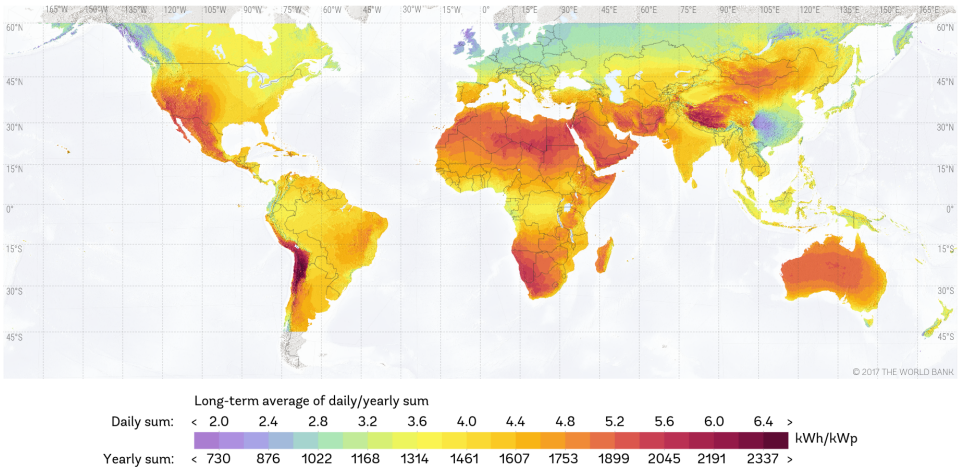

Figure 1: Chile's Photovoltaic Power Potential (kWh/kWp)

Notes: This graph shows Chile's photovoltaic power potential that refers to how much energy (kWh) is produced per kilowatt peak (kWp) of a system. Graph was retrieved from `https://globalsolaratlas.info`. Solar resource data was obtained from the *Global Solar Atlas*, owned by the World Bank Group and provided by Solargis.

on generation from thermal plants and on human health in northern Chile. By exploring the case of Chile, we add to the scant literature on power plant pollution exposure and health impacts in emerging economies (Gupta and Spears, 2017; Barrows et al., 2018).

Our study uses data on solar generation between 2012 and 2017. To identify the effects of this increasing solar expansion, we first estimate the extent to which solar plants displace other power facilities using daily variation in plant-level power generation capacity.[2] For solar generation to have a positive effect on health outcomes, it must first displace generation by thermal plants, thereby reducing pollution levels from the baseline.[3] After identifying the set of displaced thermal power plants, we estimate a reduced form equation on the effect of daily solar generation on health. In particular, using a set of zero-inflatd negative binomial (ZINB) regressions, we measure health effects using data on daily hospital admissions of patients with diagnoses associated with cardiovascular and respiratory diseases, conditions generally related with the combustion of fossil fuels. To reduce any potential endogeneity between power generation and health as well as to take into account the transport of pollutants, we leverage our findings on fossil fuel plant displacement and identify cities that are downwind to and near these displaced plants, and run separate regressions for this subsample of cities. In

[2]Ideally, we would use plant-level emissions data. Unfortunately, publicly available emissions data in Chile are engineering estimates, rather than observed or measured data.

[3]The alternative is that solar generation rises to meet expanding demands for electricity. In this case, there would be no displacement of fossil fuel plants, and the health impacts of the energy system would remain unchanged, although health improvements would have been seen relative to a counterfactual of increased fossil fuel generation in response to increased loads.

doing so, we rely on the identifying assumption that the harmful effects of local air pollution exposure are stronger downwind of the pollution source and decrease with distance. Finally, to attribute the health effects to air quality improvements, we use additional (but limited) data on fine PM concentrations for a subset of our cities and estimate an instrumental variable approach that uses solar generation as an instrument for pollution in our health regressions.

Our results show that increased solar generation in Chile led to a displacement of daily thermal generation, particularly of coal- and gas-fired power generation. Subsequently, we find that, through this displacement, solar generation reduces cardiovascular and respiratory admissions in all cities included in our sample. Our analysis by age group indicates that these reductions are mostly observed among infants (less than 1 year old), children (ages 2–14), and seniors (age 65 and more), the most vulnerable age groups. The reductions are found primarily after short-term exposure to abated pollution from displaced thermal plants, and in cities that are either downwind of these displaced facilities or that have fossil fuel generators within their borders. Specifically, we find that a full displacement of fossil fuel plants by solar would reduce respiratory hospitalizations by 6.7 percent across all cities, and by 10.6 percent in cities that are downwind and close to the displaced plants.[4] Our broad conclusions of the benefits of solar on health remain unchanged after several robustness checks, which include alternative estimation methods, the use of cities upwind of displaced facilities and those downwind of nondisplaced units, and the use of hospital admissions of patients with diseases presumably not related to air pollution.

Several reasons lead us to consider our findings as a lower bound on the true health benefits from solar generation, particularly in developing countries. First, our area of study (Chile's northern region) has limited healthcare infrastructure. Therefore, any reduction in hospitalizations can have a beneficial spillover effect by increasing the number of hospital beds available in turn helping reduce the number of untreated unrelated injuries and illnesses. Second, reductions in air pollution exposure for young children and infants have a lifelong benefit in terms of reduced illnesses and improved economic outcomes (Currie et al., 2014). Third, communities with greater shares of low-income households and minorities may live closer to large air polluters in Chile, as has been demonstrated in both the U.S. and India (Banzhaf et al., 2019; Kopas et al., 2020).[5] In this case, improvements in air quality may

[4]Results from Table 4, columns 2, statistically significant coefficients.

[5]Previous evidence shows indications that lower income populations in Chile are more likely to live near environmental disamenities, such as mining. For example, Rivera (2020) finds that residential properties near mining sites in northern Chile have lower values and that these values are particularly salient for new residents in the area, suggesting an environmental-based sorting. These inequities may also be caused by housing siting decisions; for example, Rau et al. (2015) shows evidence of government housing projects built in close proximity to mining waste sites in the city of Arica, also located in northern Chile.

not only bring greater long-term benefits to populations experiencing uneven exposure to air pollution but also help to reduce inequities caused by pollution exposure.

A wide number of papers document the displacement of coal-fired power plants, either through a decline in the price of natural gas (Lu et al., 2012; Linn et al., 2014; Knittel et al., 2015; Cullen and Mansur, 2017; Holladay and LaRiviere, 2017; Linn and Muehlenbachs, 2018; Johnsen et al., 2019), through the expansion in renewable generation capacity (Kaffine et al., 2013; Cullen, 2013; Novan, 2015; Callaway et al., 2018; Fell et al., 2021; Bushnell and Novan, 2021), or through interaction between the two (Holladay and LaRiviere, 2017; Fell and Kaffine, 2018). These studies also document significant interactions among competing renewables, whereby solar generation can lead to a shift in the supply of hydropower. To the extent that renewables offset and displace one another, the injection of new renewable sources into the grid may lead to ambiguous environmental impacts. One of the benefits of conducting this analysis in northern Chile is the small amount of non-solar renewables on the grid during the study period (contributing only 6% of total capacity in 2017, combined). This allows us to isolate the effect of solar generation on fossil fuel displacement more clearly.

We extend this previous literature by empirically documenting some of the consequences of the displacement on morbidity outcomes. A small subset of literature estimates the effect of changes in the power sector on health. For example, Burney (2020) estimates the health benefits associated with the shift from coal to natural gas combustion in the U.S., finding that the exit of coal-fired plants between 2005 and 2016 saved approximately 26,000 lives. Along those lines, Casey et al. (2018a) find that coal and oil power plant retirement in the U.S. led to improvements in fertility outcomes, and Casey et al. (2018b) show the link between these retirements and a decrease in preterm births among nearby populations. Our work adds to this literature, presenting new evidence on the benefits that curtailing coal-fired generation has on morbidity. Moreover, we estimate this impact even without coal plant retirement; rather, we can identify the health benefits of having a large amount of solar generation at the intensive margin, even if it does not lead to coal plant shutdowns. In doing so, we contribute to the literature by quantifying the value of curtailing coal-fired generation.

The analysis of solar generation also represents an advantage in evaluating the health benefits of renewables relative to other similar sources such as wind. Increases in wind power generation may be associated with reduced pollution due to higher wind speeds and greater dispersion, hampering the identification of health impacts. There is existing work identifying the health benefits of a cleaner grid (Anenberg et al., 2012; Muller and Mendelsohn, 2009) or the addition of new utility-scale solar capacity (Sergi et al., 2020) in integrated assessment frameworks. The latter employs cutting-edge air transport and chemical transformation models but uses existing epidemiological literature and underlying health and population

statistics to calculate the impact of policies on health. To the best of our knowledge, we are the first to *empirically* test the impact of increased large-scale solar generation on health. Therefore, our work also adds to the growing literature on the co-benefits of renewable generation (Siler-Evans et al., 2013; Barbose et al., 2016; Buonocore et al., 2016; Spiller et al., 2017; Millstein et al., 2017), a key aspect in evaluating the economic potential of renewable energy portfolios (Edenhofer et al., 2013; Wiser et al., 2017; Hollingsworth and Rudik, 2019), and in the design of health-based air quality regulations (Abel et al., 2018; Thakrar et al., 2020).

The remainder of our work proceeds as follows. We review the literature on the health effects of power plant emissions in Section 2, demonstrating that emissions from thermal power generation can cause a variety of different negative health impacts, with major morbidity impacts on respiratory and cardiovascular outcomes—the two health outcomes on which we focus. In Section 3, we describe the power sector in Chile detailing the aspects of the independent northern grid we are studying in this paper as well as describing how plants are dispatched, which helps inform our displacement analysis. We explain the data in Section 4, including data on health outcomes, power plant generation, wind directions, and control variables such as demographic information. Our empirical strategy is detailed in Section 5, as well as our identification approach, which relies upon wind direction and the results from our displacement analysis to identify downwind cities. The results and robustness checks are in Sections 6 and 7, respectively, where we show that solar can effectively displace thermal power generation and improve health outcomes, particularly in downwind cities, and that our results are robust across different methodologies and approaches. Finally, we conclude in Section 8 with a discussion about the policy implications of our findings.

2 Power Plants' Emissions and Health Consequences

Fossil-fuel electricity generation accounts for a large share of greenhouse gas emissions, particularly carbon dioxide (CO_2), an important contributor to global warming and climate change (Stocker et al., 2013). The sector is also a major driver of outdoor air pollution, primarily due to the burning of coal, which releases important amounts of airborne pollutants such as sulfur dioxide (SO_2), nitrogen oxides (NO_X), mercury (Hg), and particulate matter (PM). All of these pollutants are associated with adverse health effects, mortality risks and threats to life expectancy (Chay and Greenstone, 2003a,b; Currie and Neidell, 2005; Bateson and Schwartz, 2007; Currie et al., 2009; Chen et al., 2013; Arceo et al., 2016; Knittel et al., 2016; Schlenker and Walker, 2016; Lavaine and Neidell, 2017). Coal combustion also affects water quality. Ash released after coal combustion can end up in water reservoirs,

contaminating waterways and sources of drinking water (Carlson and Adriano, 1993). Here, we briefly summarize the evidence on the detrimental health impact of exposure to the main pollutants from coal combustion. Evidence suggests that its displacement by solar generation is expected to curtail mostly SO_2, PM, and NO_X emissions.

SO_2 is an invisible gas, part of the sulfur oxide (SO_X) family of gases, formed when fuel containing sulfur (e.g., coal, oil) is burned (U.S. Environmental Protection Agency, 2014). Exposure to high concentrations of this pollutant is associated with eye, nose, and throat irritation, infectious complications of chronic obstructive pulmonary disease, and increases in hospital admissions due to obstructions of the lower airway (e.g., asthma) (World Health Organization, 2006). SO_2 reacts with other compounds in the atmosphere to form fine PM. PM is the general term used to describe solid particles, dust, and drops found in the air, all with different compositions and sizes. Evidence on the health impact of exposure to coarse PM (PM_{10}) and fine PM ($PM_{2.5}$) suggests detrimental effects on a variety of health outcomes, including respiratory diseases (Schwartz, 1996; Coneus and Spiess, 2010), cardiovascular diseases (Schwartz and Morris, 1995; Brook et al., 2010; Franklin et al., 2015), low birth weight (Currie et al., 2009; Coneus and Spiess, 2010; Currie and Walker, 2011), and infant mortality (Chay and Greenstone, 2003a,b; Arceo et al., 2016; Knittel et al., 2016).

NO_X are reactive gases and include nitrogen dioxide (NO_2), nitrous acid (HNO_2), and nitric acid (HNO_3). Although mobile sources are responsible for the highest domestic anthropogenic release of NO_X into the atmosphere, stationary fossil fuel combustion represents a significant portion of annual domestic NO_X emissions. Outdoor exposure to NO_X has been found to increase asthma and bronchitis diagnoses in children (Orehek et al., 1976; Pershagen et al., 1995; Chauhan et al., 2003; Gauderman et al., 2005), and on older populations (Schlenker and Walker, 2016). This pollutant can also react in the presence of heat and sunlight in the atmosphere to create ground-level ozone, a harmful chemical associated with lung diseases and premature deaths (Bell et al., 2004, 2005).

Evidence on the health impact of exposure to power plant pollution is limited within the Chilean context. Epidemiological research from Ruiz-Rudolph et al. (2016) show significantly higher rates of cardiovascular and respiratory hospital admissions in Chilean municipalities that host power plants and other large-scale polluters. However, the authors fail to take into account proximity to the pollution source, or the air transport of pollutants in the vicinity of these facilities. This further highlights the importance of our work—identifying a causal impact of exposure to power plant pollution on respiratory and cardiovascular hospitalizations in Chile by relying on an exogenous source of variation: the incremental increase in solar electricity generation capacity over time.

3 The Power Sector in Chile

The electricity sector in Chile is composed of three different segments: generation, transmission, and distribution, all 100% privately owned. The sector is dominated by fossil fuels, which account for 53% of total generation, followed by hydro with 28%. The fossil fuel generation mix is primarily coal (40%), followed closely by natural gas (36%) and petroleum (24%) (Comisión Nacional de Energía, 2018).

Before 2018, Chile's electricity market featured four different electric systems (see Appendix Figure A1): two major interconnected systems, the Northern Interconnected System (Sistema Interconectado del Norte Grande — SING) and the Central Interconnected System (Sistema Interconectado Central — SIC); and two additional minor grids, the Aysen Electric System (Sistema Eléctrico de Aysen — SEA) and the Magallanes Electric System (Sistema Eléctrico de Magallanges — SEM). The SING system, located in Chile's northern region, has 5 GW of installed capacity, 2.5 GW of peak load, and more than 85% reliance on fossil fuel generation (i.e., coal, natural gas, and diesel). Although the northern region of Chile is relatively unpopulated, with SING serving only 7% of the country's total population, this region hosts most of the large-scale copper mining companies that operate in the country, a sector characterized by its electricity-intensive production activities.[6] Conversely, the SIC system, located in central-south Chile and with 17 GW of total installed capacity and 7 GW of peak load, relies heavily on hydro generation (around 35%) and serves 90% of the country's population. These two major grids, SING and SIC, began an interconnection process in November 2017 that resulted in a full integration by May 2019, thereby creating Chile's National Electric System (Sistema Eléctrico Nacional — SEN). In this paper, we focus on the period before November 2017, thus avoiding any potentially confounding factors that may be associated with the interconnection itself.

3.1 The Generation Segment

Electricity generation in Chile is produced in a competitive market, though the transmission and distribution sectors are regulated. Generation at SING is characterized by a spot market, long-term forward contracts, and capacity payments. The spot market relies upon merit-order dispatch under the coordination of the Economic Load Dispatch Center (Centro de Despacho Económico de Carga — CDEC), which, to meet the system's load, dispatches generators at every hour based strictly on their marginal cost. Thus, the hourly marginal

[6] During 2016, the copper industry consumed 50,578 TJ of electricity supplied by SING. This consumption was equivalent to more than 30% of SING's installed capacity of 5 GW (data retrieved in May 2020 from https://www.cochilco.cl).

cost of the system equals the cost of the most expensive unit being dispatched (Galetovic and Muñoz, 2011).[7] This dispatch, determined by CDEC based on fuel costs, informs our methodology in estimating the displacement of fossil fuel plants by solar generation. Specifically, we incorporate the relative costs of fossil fuels into our dispatch equation to control for the market forces that will play a large role in determining dispatch and the ability of solar to displace fossil fuel plants (see Section 5.1).

3.1.1 Solar Generation

Although numerous PV systems have existed in Chile since 2007, they were mostly in the form of small-scale stand-alone systems and part of rural electrification programs (Haas et al., 2018). In 2008, however, the Chilean government established a quota system for renewable energies ("Ley de Energías Renovables No Convencionales"—ERNC); this currently requires that these sources account for 20% of participation in the energy mix by 2025 (Ministry of Energy, 2013). The ERNC policy, in combination with decreasing costs in PV technology, led to the installation in 2012 of the first large-scale solar plant in northern Chile, La Huayca, adding 25.05 MW of gross capacity to SING. By 2015, solar participation at SING reached 119 MW, equivalent to 2% of the total daily system generation (≈.376 GWh). By the end of 2017, this participation had grown to 655 MW, equivalent to 10% of total daily system generation (≈1.5 GWh).[8]

3.1.2 Emissions

Due to Chile's heavy reliance on fossil fuels, the power sector accounts for approximately 40% of the nation's total greenhouse gas emissions; producing 34,568.2 kt and 1.6 kt of carbon dioxide equivalent emissions (CO_2e) due to CO_2 and methane (CH_4) discharges, respectively (Chile Environmental Ministry, 2018). In terms of criteria air pollutants, the sector accounts for more than 30% of the country's total NO_X and SO_2 emissions, two hazardous pollutants common to coal combustion (see Section 2). This situation is aggravated by the longevity of some fossil fuel power plants, as older plants generally emit more. In SING, for instance, some coal-fired generators are the oldest in the country, with ages that in some cases exceed 50 years (Programa Chile Sustentable, 2017). Annual discharges from the sector comprise 57% and 40% of the northern grid's total SO_2 and NO_X emissions, respectively (Chile Environmental Ministry, 2017).

[7] Regardless of whether generators are dispatched, each of these agents receives a monthly capacity payment aimed at guaranteeing enough generation capacity to supply energy during times of peak demand.

[8] Data retrieved from the annual reports of Chile's National Energy Commission (Comisión Nacional de Energía — CNE), https://www.cne.cl/nuestros-servicios/reportes/informacion-y-estadisticas/

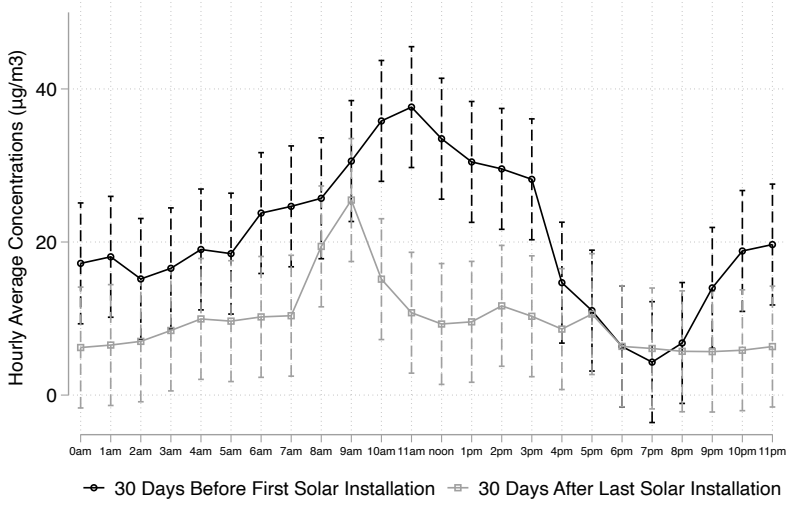

(a) SO_2

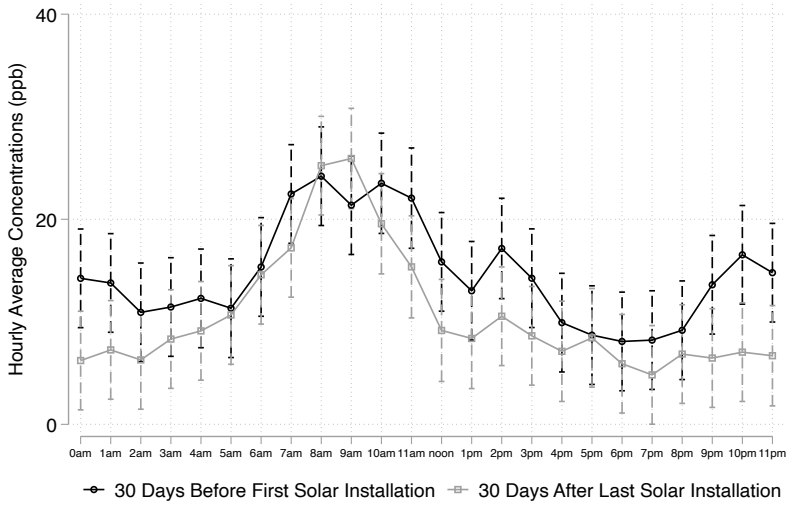

(b) NO_X

Figure 2: Hourly Sulfur Dioxide (SO_2) and Nitrogen Oxide (NO_X) Average Concentrations in Tocopilla Before and After the First Solar Connection

Notes: This figure shows point estimates and 95% confidence intervals for hourly average concentrations in the city of Tocopilla 30 days before and 30 days after the first and last solar power connections. Point estimates are obtained after regressing hourly concentrations averaged across stations on dummies for hour interacted with an indicator taking the value of 1 for observations after the last solar connection, and 0 for observations before the first solar connection. Hourly predictions "30 days before the first solar connection" correspond to observations before October 1st, 2012. Hourly predictions "30 days after the last solar connection" correspond to observations after July 21st, 2017. SO_2 is measured in micrograms per cubic meter of air ($\mu g/m^3$), and NO_X in parts per billion (ppb). Data come from the Ministry of Environment through the National Air Quality Information System (SINCA). From the original data, we trim the top and bottom 1% of all observations.

Data on NO_X and SO_2 at the city level are limited in the country. For the cities in our analysis, only the city of Tocopilla—the city with the highest number of coal-fired power plants in SING—has a monitoring station that records NO_X and SO_2. Figure 2 plots the hourly average SO_2 (a) and NO_X (b) concentrations in this city, 30 days before the first solar connection in our sample (black line), and 30 days after the last one (gray line). Relative to the situation before the first solar connection, panel (a) of Figure 2 shows a statistically significant decrease in hourly SO_2 concentrations right after all solar plants were connected into the system particularly during the hours in which solar panels are at peak capacity (between 10 a.m. and 3 p.m.). A similar trend is observed in panel (b) for NO_X, although the difference in concentrations before and after seems to lack statistical significance. The extent to which the reductions observed for SO_2 in Figure 2 are effectively due to the entry of new solar installations anticipates the potential positive health impact of a cleaner grid.

Regarding PM, Chile generally registers high levels of daily average $PM_{2.5}$ concentrations.[9] In the northern part of the country, these levels are largely due to the region's dependence on fossil fuel power generation (Chile Environmental Ministry, 2017).[10] As with other pollutants, $PM_{2.5}$ data at the city level are sparse, with only four cities of our subsample reporting the concentrations. Figure 3 depicts daily average $PM_{2.5}$ concentrations between 2010 and 2019 across the four cities in our sample with available data. In dashed red, we include the WHO's air quality standard of 25 $\mu g/m^3$ for 24-hour averages as a reference. As shown, daily average concentrations seem to have decreased over time but still exceed air quality standards during certain times of the year.[11] This situation highlights the importance that solar-powered electricity can play in reducing environmental-related health concerns in areas with a heavy reliance on fossil fuels.

Preferably, we would test the main hypothesis of this paper using data similar to those in Figures 2 and 3. As mentioned earlier, however, we lack comprehensive city-level data on airborne pollution concentrations for all the cities in our sample, as air quality monitoring stations in Chile are scarce for cities other than Santiago. We address this limitation with our displacement analysis, effectively proxying for changes in emissions due to changes in fossil fuel-based generation. Later in the paper, we employ the available data on $PM_{2.5}$ concentrations for the four cities in our sample as an additional test on our results (see

[9] Previous studies have documented some of the harmful effects of PM exposure in Chile. For instance, Dardati et al. (2021) show that increases in $PM_{2.5}$ lead to a rise in respiratory emergency-room visits, while Bharadwaj et al. (2017) expose some of the long-term harmful effects of early-life exposure to CO (and PM) on cognitive performance.

[10] The power sector is also the largest emitter of direct discharges of pollutants into the ocean and coastal waters in Chile's northern region (Chile Environmental Ministry, 2017).

[11] In particular, a total of 199 days between 2012 and 2017 exceed 25 $\mu g/m^3$, which is equivalent to 9.29% of the days in Figure 3.

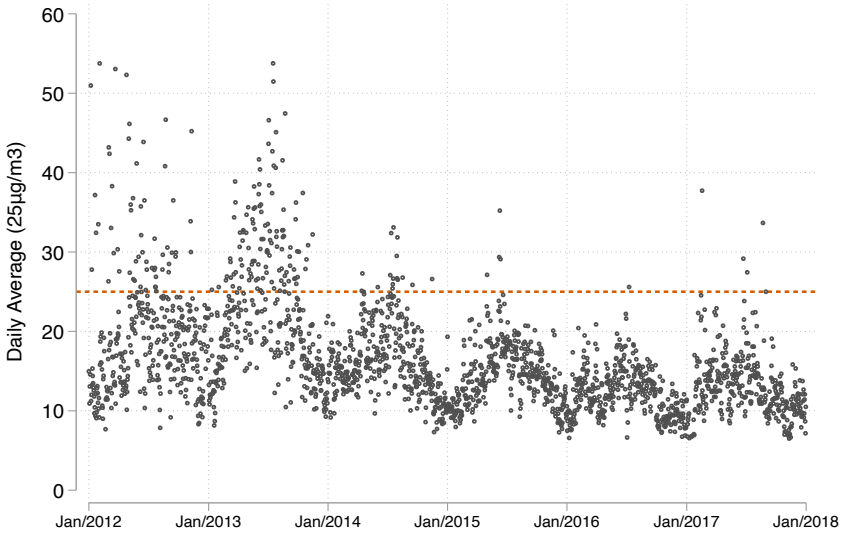

Figure 3: Daily Average $PM_{2.5}$ Concentrations at SING

Notes: This figure shows daily average fine particle matter ($PM_{2.5}$) concentrations across cities at SING hosting thermal power plants from 2012 to 2018. Observations are in $\mu g/m^3$. The dashed-red reference line represents the World Health Organization's 24-hour mean guideline of 25 $\mu g/m^3$. We trim the top and bottom 1% of all observations. Data come from the National Air Quality Information System (Sistema de Información Nacional de Calidad del Aire — SINCA) from 2012 to 2017.

Section 6.2.2).[12]

4 Data

4.1 Plant-Level Data

We obtain comprehensive plant-level data on daily power generation from the National Electricity Coordinator (Coordinador Eléctrico Nacional — CEN), the national body in charge of SING. Along with the information on generation, the data include specifics on plant-level technology and capacity, which we later merge with data on fuel use and prices obtained from the National Energy Commission (Comisión Nacional de Energía — CNE). As November 2017 was the month in which SING and SIC were first connected, our study periods goes from 2012 until 2017. Descriptive statistics for daily generation by energy source are presented in Table 1, while fuel use and prices are in panels A and B, respectively, of Appendix Table A1.

[12]Another possibility would be to include emissions at the facility level, to test the effect of solar on emissions at the plant. However, the emissions data that are collected by the government are not observed data, rather, they are engineering estimates based on generation (thus, they are a simple transformation of the kWh generated in each hour). Due to this data limitation, we utilize generation as a proxy for emissions.

Table 1: Daily SING Generation (GWh) by Plant Primary Fuel Source

Energy Source	Obs.	Mean	Std. Dev.	Min.	Max.	Initial Year: 2012		Final Year: 2017	
						#EGUs	Cap. (MW)	#EGUs	Cap. (MW)
Coal	2,192	39.36	3.68	17.62	49.04	13	1,959	15	2,449
Diesel	2,192	.12	.19	0	1.99	12	117	13	117
Fuel oil	1,187	0.07	0.12	0	0.63	3	36	3	36
Fuel oil #6	2,192	0.37	0.49	0	2.30	4	177	7	50
Natural gas	2,192	5.03	2.18	0	17.29	5	1,368	6	1,925
Hydro	2,192	0.21	0.03	0.07	0.33	4	16	5	17
Geothermal	306	0.21	0.20	0	0.73	-	-	2	79
Wind	1,492	.84	.47	0	2.78	-	-	2	200
Solar	1,918	1.46	1.60	0	6.09	1	25	18	655

Notes: This table displays main descriptive statistics on daily power generation at Chile's northern grid, SING, from 2012 to 2017. The information is displayed by primary fuel source. Observations are plant-days. EGUs are electric generating units. Capacity (cap.) is the average net capacity for the given year. All gas-fired power plants are combined-cycle (CC) plants that also run with diesel. Data come from the National Electricity Coordinator from 2012 to 2017.

Table 1 shows that coal-fired electric generating units (EGUs) are SING's main source of power generation, with an average of 39.36 GWh per day, followed by gas-fired units with 5.03 GWh, and solar units with 1.46 GWh. This is consistent with the amount of fuel used by these sources, as coal and gas plants report the greatest usage in Table A1. From Table 1, we also observe that coal-fired and hydroelectric plants are always dispatching in our sample, as revealed by the positive minimum daily generation. Furthermore, solar generation experienced the highest growth in terms of the number of new units and capacity installed into the system, as shown in the last four columns of Table 1.[13]

Figure 4 depicts the share of SING's monthly power generation by both fossil fuel and solar facilities during the sample period. At the start of the period, power generation at SING was (almost fully) coming from fossil fuels, with coal alone representing around 85% and natural gas roughly covering the other 15%. Although there was some solar generation by the end of 2012, a significant injection of solar-generated energy started at the beginning of 2015. As shown in the same figure, this injection coincides with the persistent decrease in fossil fuel power generation over the same period. By the end of 2017, coal-generated electricity represented around 77% of SING's monthly generation, while natural gas use was

[13]Note in Table 1 that the total net capacity of plants running with fuel oil #6 decreased from 177 MW in 2012 to 50 MW in 2017. This is due to the closure of two main generators, units U10 and U11, part of Termoelectrica Tocopilla, a power plant in operation since 1960. Four generators indeed were closed during the sample period. Although solar generation may also displace fossil fuel generation at the extensive margin, our main analysis is conservative as it is centered around the effects of displacement at the intensive margin only. If these shutdowns were a consequence of the injection of solar power into the system, our estimates would thus constitute a lower bound of the true effect of solar power generation on improved health outcomes.

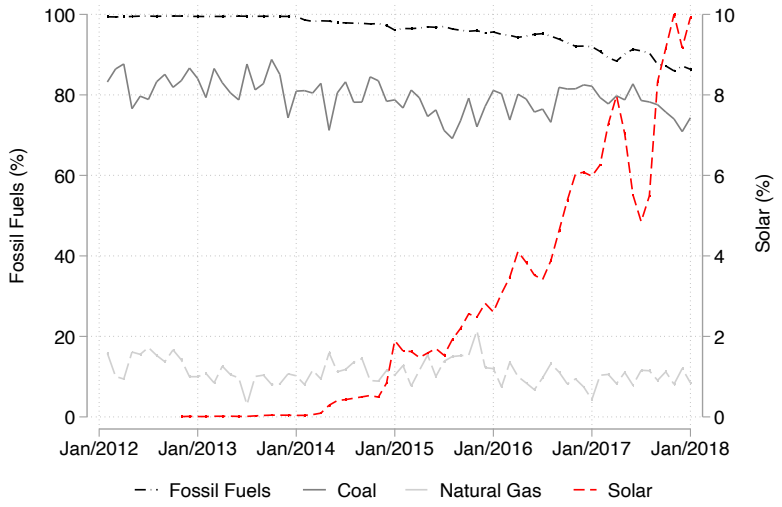

Figure 4: SING's Monthly Fossil Fueled and Solar Power Generation

Notes: This figure shows monthly power generation at Chile's northern grid, SING, by fuel source from 2012 to 2017. Data are reported in percentages relative to SING's monthly generation. Fossil fuels' monthly generation is shown in the main y-axis. Solar monthly generation is shown in the secondary y-axis. Data come from the National Electricity Coordinator from 2012 to 2017.

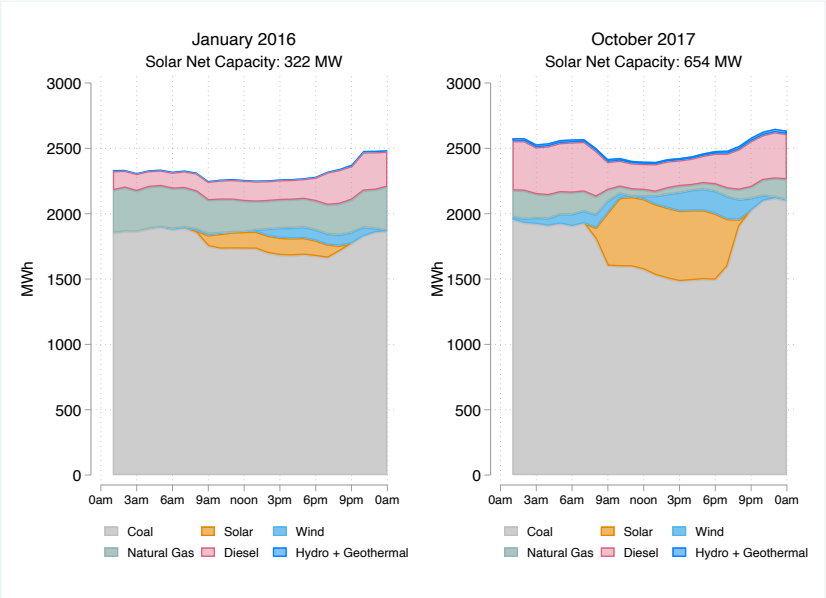

Figure 5: SING's Hourly Generation by Fuel Before and After Large-Scale Solar Installations

Notes: This figure shows SING's total hourly generation by fuel source before and after large-scale solar power generation investments. The left-hand side graph shows hourly generation (in MWh) by fuel averaged over the first week of January 2016 (with 322 MW of net solar capacity). The right-had side graph shows hourly generation (in MWh) by fuel averaged over the last week of October 2017 (with 654 MW of net solar capacity). Data come from the National Electricity Coordinator from 2016 to 2017.

equivalent to less than 10%.[14]

A more detailed overview of the relationship between solar and other fuels is offered by Figure 5, which depicts SING's hourly generation by fuel source averaged over the first week of January 2016 (left-hand side), and the last week of October 2017 (right-hand side), just before the SING–SIC interconnection.[15] Starting in 2016, SING had nine solar plants with 332 MW of total net capacity actively injecting power to the grid. By October 2017, this capacity had doubled to 18 active solar projects, with a total net capacity of 654 MW. When comparing these two periods in Figure 5, we observe that this increased solar capacity largely displaced hourly coal- and gas-fired combustion during Atacama's sunlight hours (7 a.m.–7 p.m.).

4.2 Health Outcomes

We use data from the Department of Health Statistics and Information (Departamento de Estadísticas e Información de Salud — DEIS), part of Chile's Ministry of Health, from 2012 to 2017. DEIS provides data on each patient that has been discharged from any hospital in the country, together with information on their date of admission, age, and the physician's diagnosis of the leading cause of disease based on International Standard Classification (ICD-10). Although the data are compiled at the hospital or urgent care center level, they include a variable on each patient's city of origin. This allows us to construct a panel of city-level daily hospital admissions, which constitutes our main health outcome. We focus on hospital admissions due to cardiovascular (codes I00/I999) and respiratory conditions (codes J00/J999), and, within respiratory conditions, we further examine upper and lower respiratory infections.[16] Descriptive statistics on the daily rate of hospital admissions by admission condition are presented in panel A of Table 2 for the 19 cities in the sample.

In addition to constructing health outcomes by disease, we also compile health outcomes across age groups using the patient's age. In particular, we examine morbidity outcomes

[14]Appendix Figure A2 shows SING's total monthly load over the sample period (dashed line). The increasing trend in demand over time indicated in this graph rules out a demand-driven reduction in fossil fuel power generation. The Figure also shows that SING's total monthly solar generation (solid line) has increased at a faster rate than demand over the same period.

[15]Unfortunately, publicly available hourly generation data start in 2016.

[16]Specifically, we use codes J00/J069 and J30/J399 for upper respiratory, and codes J09/J189 J20/J229 J40/J479 J60/J709 J80/J869 for lower respiratory diseases. Upper respiratory infections affect the nose and throat, causing symptoms such as sneezing and coughing. Among the most frequent upper respiratory infections are the common cold, sinusitis (sinus inflammation), epiglottitis (trachea inflammation), and laryngitis (infection of the voice box). Lower respiratory infections affect the lungs and lower airways. Common lower respiratory infections are bronchitis (bronchial tube inflammation), bronchiolitis (an infection of the small airways, affecting children), pneumonia (a lung infection), asthma (long-term disease of the lungs), influenza, and tuberculosis (bacterial lung infection).

Table 2: Summary Statistics on the Daily Rate of Hospital Admissions

Disease	Mean	Std. Dev.	Min.	Max.	Obs.
Panel A. All Cities					
Cardiovascular	1.044	4.848	0	409.84	41,648
All respiratory	1.204	5.636	0	409.84	41,648
Upper respiratory	0.274	2.002	0	168.35	41,648
Lower respiratory	0.787	4.363	0	319.49	41,648
Panel B. Downwind Cities $\leq$ 10km of Displaced Plants					
Cardiovascular	2.253	3.114	0	21.75	4,384
All respiratory	2.552	4.069	0	57.92	4,384
Upper respiratory	0.482	2.550	0	57.15	4,384
Lower respiratory	1.854	2.893	0	24.13	4,384
Panel C. Downwind Cities $\leq$ 50km of Displaced Plants					
Cardiovascular	1.818	3.002	0	21.75	6,576
All respiratory	2.029	3.707	0	57.92	6,576
Upper respiratory	0.379	2.175	0	57.15	6,576
Lower respiratory	1.478	2.737	0	24.13	6,576
Panel D. Downwind Cities $\leq$ 100km of Displaced Plants					
Cardiovascular	1.545	3.082	0	30.13	8,768
All respiratory	1.692	3.635	0	57.92	8,768
Upper respiratory	0.314	2.009	0	57.15	8,768
Lower respiratory	1.244	2.784	0	30.18	8,768

Notes: This table displays main descriptive statistics on the daily rate of hospital admissions (all ages) by disease from 2012 to 2017. Hospital admission rates are per 100,000 people. We separate out the sample by all cities, and then specifically for those cities downwind of displaced thermal plants (identified in Section 6.1), at different distances. Data come from the Ministry of Health, through the Department of Health Statistics and Information (DEIS) from 2012 to 2017.

across infants (< 1-year old), toddlers (between 1- and 5-years old), kids (between 6- and 14-years old), adults (between 15- and 64-years old), and seniors (65-years old or more). Descriptive statistics on the daily rate of hospital admissions by age group are in Appendix Table A2.

4.3 Wind Direction

Our data on wind direction come from Chile's Meteorological Service and Air Quality System from 2012 to 2017. The data cover four cities that host fossil fuel power plants,

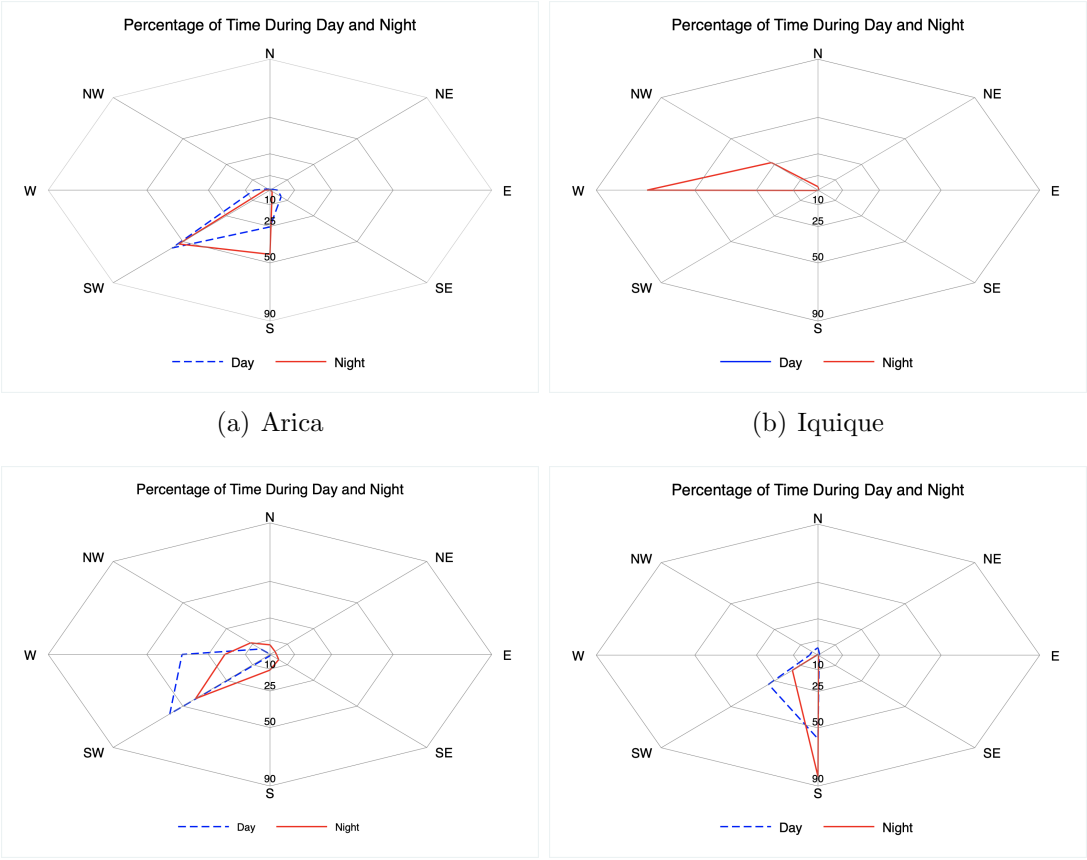

(a) Arica (b) Iquique

(c) Tocopilla (d) Antofagasta

Figure 6: Daily Wind Direction in Cities with Fossil Fuel Generation

Notes: This figure shows daily wind directions in four (out of five) cities that host fossil-fueled generators in our sample. "Daytime" (dashed line) encompasses average wind direction patterns during sunshine hours (7 a.m.–7 p.m.). "Night" (solid line) encompasses average wind direction between 7 p.m. and 7 a.m. the following day. Concentric circles represent the percentage of time in which the wind blows in that direction, namely 10%, 25%, 50% and 90%. Data come from the Meteorological Service and Air Quality System from 2012 to 2017. Data on daytime wind direction for Iquique (Panel 6(b)) are not available.

namely Arica, Iquique, Tocopilla, and Antofagasta.[17] The eight-wind compass roses for these cities are displayed in Figure 6 for daytime (dashed line) and nighttime (solid line) wind patterns for all cities except for the city of Iquique (in Figure 6(b)), for which we only have nighttime wind direction. In the definition of downwind cities, we approximate daytime wind patterns for Iquique using nighttime information. Although wind speed is generally higher at night, we use daytime information given our focus on the daily thermal displacement by solar energy sources. Considering that solar installations produce at peak capacity around midday, we expect daytime wind direction patterns to be more informative

[17]Mejillones is another city with fossil fuel power plants but no available wind data; instead, we rely on information from the nearest available city, Antofagasta, 62 km away.

of a population's true exposure to reduced emissions from the displacement of fossil fuel generation during solar availability.

4.4 Other Covariates

We also obtain information on other factors potentially correlated to hospital admissions. First, we obtain data on city-level demographic characteristics such as population, density, poverty and fertility rates as a proxy for socioeconomic factors known to affect health outcomes.[18] We gather this information from the National System of Municipal Information (Sistema Nacional de Información Municipal — SINIM). The demographic data are updated every two years, and therefore we can include these variables in our estimation regressions jointly with city-fixed effects.

Data on weather come from two different sources. First, we gather information on maximum and minimum temperatures from the National System on Water Information (Sistema Nacional de Información del Agua — SNIA) for several monitoring stations located in remote areas in northern Chile. Although we obtain this information for almost all cities in our dataset, there are some incomplete entries, which we replace with daily regional averages. The second source is Solar Explorer, an initiative of the Chilean Ministry of Energy (Ministerio de Energía) that contains data on humidity for all the cities in our sample. Descriptive statistics for these covariates are in Panel A of Table A3 in the Appendix.

5 Methods

5.1 Displacement

We begin by econometrically identifying the effect of solar adoption on the power generation of existing power plants from 2012 to 2017.[19] To that end, we categorize all the plants in the system by their primary fuel type (e.g., coal, diesel, natural gas, fuel oil) and then define a set of linear models of daily generation to estimate which types of plant decrease or increase their production with the introduction of solar generation. Given our interest in the overall effect of solar power generation on health, we use daily-level variation in generation to identify effects because total daily generation (and thus emissions) is more directly related to health outcomes than, say, hourly shifts. We define our baseline aggregated generation displacement equation as follows:

[18] Unfortunately, city-level data on indicators such as unemployment and income are not publicly available.

[19] Our displacement analysis is a short- to medium-term analysis given that it takes SING's infrastructure as given during our sample period (Baker et al., 2013).

$$G_d^f = \gamma_0 + \gamma_1 S_d + \sum_{j \neq f} \delta^j \left(FuelUse_m^f * \frac{P_m^f}{P_m^j} \right) + \gamma_2 Load_d + \omega_d + \tau + \epsilon_d^f, \quad (1)$$

where G_d^f is the system's generation by fuel f during day d, ω_d is a vector of daily weather covariates, τ is a vector of time-fixed effects, and ϵ_d^f is an error term. We consider two options of τ. The first, τ_1, includes year, month, and weekend fixed effects, while a stronger version, τ_2, includes year, seasons, year $\times$ seasons, and weekend fixed effects.

Equation (1) also includes the variable $Load_d$ that represents the system load during day d to control for increases in demand over time, as demonstrated by Appendix Figure A2.[20] In addition, Equation (1) considers a term that models SING's dispatch of generators to control for differences in input prices that may affect daily dispatch conditions. This term is given by the interaction between aggregate use of fuel f during month m, $FuelUse_m^f$, and the relative international (exogenous) monthly prices of the fuels in the system, P_m^f/P_m^j, where $f \neq j$. Importantly, we do not include relative prices with respect to solar energy or other renewables, given their zero marginal cost.

The key variable in Equation (1) is S_d, which represents the system's solar generation during day d. The idea behind this specification is that, after controlling for plant-level (fuel use) and system-specific covariates (prices, load), weather, and time fixed-effects, residual variation in generation by fuel f can be explained by variation in the system's total solar power generation. Thus, the parameter γ_1 reflects whether and to what extent solar power generation induces a significant change in generation by non-solar sources. A negative (positive) γ_1 will signal a solar-induced displacement (ramp-up) of non-solar sources.

We estimate Equation (1) with an ordinary least square (OLS) estimator, bootstrapping the standard errors to account for any heterogeneity and serial correlation in the generation data. To take into account the heterogeneous capacity across fuel types, we also estimate an alternative specification of Equation (1) in which we replace G_d^f by capacity factor CF_d^f, defined as the total daily generation by fuel f weighted by its net capacity. Given that CF_d^f takes values between 0 and 1, we estimate this version of Equation (1) using a generalized least-squares (GLM) estimator assuming a logit distribution.

Alternatively, we run a plant-level version of Equation (1) to individually identify the set of plants displaced by solar generation and those that are not. In this case, we modify Equation (1) to include generation G_{id}^f at plant i, and the plant's corresponding fuel use

[20] As the large-scale copper mining industry is an important agent in the demand for energy at SING, variations in daily load should also capture similar variations in copper production.

$FuelUse^f_{im}$, as follows:

$$G^f_{id} = \beta_0 + \beta_1 S_d + \sum_{j \neq f} \delta^j \left(FuelUse^f_{im} * \frac{P^f_m}{P^j_m} \right) + \beta_2 Load_d + \omega_d + \tau + \epsilon^f_{id}. \quad (2)$$

5.2 Solar Generation and Health

Once we have identified whether solar power generation induced a displacement of fossil-fueled plants, our next step is to estimate the effect of solar power generation on hospital admissions. We define our baseline health equation as follows:

$$Health_{jd} = \delta_0 + \delta_1 S_d + \delta_2 pop_j + \omega_{jd} + \zeta + \tau + \nu_{jd}, \quad (3)$$

where $Health_{jd}$ represents a health outcome in city j during day d; pop_j is city j's population; ω_{jd} is a vector of daily city-level weather covariates that may affect morbidity outcomes such as daily maximum and minimum temperatures and humidity; ζ is a vector of city-fixed effects (or city $\times$ year fixed effects); τ is a vector of time-fixed effects; and ν_{jd} is an idiosyncratic effect. Unlike Equation (1), here we use the strongest specification of time-fixed effects, which includes year, seasons, year $\times$ seasons, and weekends (that is, vector τ_2).

The main variable in Equation (3) is S_d, which measures SING's total solar generation on day d. Because we construct this variable utilizing generation from all solar plants in the system, daily variation in S_d is exogenous to any daily variation in hospital admissions in a given city j, and thus, our parameter of interest, δ_1, gives us an unbiased estimate of the marginal effect of daily solar generation on daily hospital admissions. We estimate Equation (3) with a maximum likelihood estimator assuming a Zero-Inflated Negative Binomial (ZINB) distribution. To interpret our coefficient estimates as rates, we restrict the coefficient of the population size (δ_2) to one. We opt for a ZINB regression due to a large number of zeros in the outcomes (count variables) and a clear overdispersion of these outcomes across cities in our sample, which make other distributions (e.g., Poisson) less suitable for our data.[21] Later in the paper, however, we test the robustness of this decision by estimating a Negative Binomial, a Poisson, and an OLS regression.

There are some potential drawbacks in the estimation of Equation (3). First, fossil fuel plants are not randomly placed across the region, so cities with and without fossil fuel plants may be observably different. Indeed, this is the case exhibited in panels B and C of Appendix Table A3, which show that cities without fossil fuel plants (panel C) are smaller, less dense, and with higher poverty rates than those with fossil fuel plants (panel B) (all

[21] See Figure A3 (Appendix) for an example of the overdispersion and the pile-up-at-zero characteristics present in our data.

of these differences are statistically significant). Thus, in addition to city-fixed effects, we also control for time-varying demographic characteristics (e.g., poverty rate, density, fertility rate) in the estimation of Equation (3). Second, the large copper mining industry is an important agent in the demand on the energy sector in northern Chile, and also a significant air pollution emitter. For this reason, we also include monthly large-scale copper production by city in the estimation of Equation (3).[22]

Third, there may be substantive dynamic effects of daily avoided fossil-fueled pollution on health outcomes. As air pollution gathers and accumulates in the atmosphere over time, we would expect to see a lagged impact of daily improvements in air quality on health.[23] In particular, air quality improvements over three or four days may very well lead to more significant health benefits today than contemporaneous improvements in air quality. In that case, Equation (3) would give us an incomplete picture of the actual health effect of a cleaner grid.

There is precedent in the literature for testing the effect of lagged exposure to air pollution on health. For instance, Neidell (2009) includes up to six days of lags (with only four days of lags in their preferred specification), while Schlenker and Walker (2016) opt for three days of lags. Although these two studies are looking at *degradation* of air quality while we look at *improvements* in air quality, we could potentially identify a dynamic effect by including lags in our health equation. However, this is not straightforward in our setting because our variable of interest (solar generation) is highly colinear across days.[24] Thus, including lags and leads would result in unstable estimates due to the multicollinearity of the variables. Instead, we take a slightly different approach by testing whether there is a cumulative impact of longer-term solar generation (and thus, longer periods of exposure to reduced fossil fuel-related pollution) on health. We do this by estimating the impact of average weekly, monthly, and yearly solar generation on health outcomes, as depicted by Equation (4) where $T = \{7, 30, 365\}$. Expressed in this way, δ_{1T} approximates the average long-term effect of solar generation on daily hospital admissions.

$$Health_{jd} = \delta_0 + \delta_{1T} T^{-1} \sum_{t=1}^{T} S_{d-t} + \delta_2 pop_j + \omega_{jd} + \zeta + \tau + \nu_{jd}, \tag{4}$$

[22]Large-scale copper mining operations roughly represents 96% of the industry's total production. We obtain monthly large-scale copper production from the Chilean Copper Corporation (Corporación Chilena del Cobre — COCHILCO). We would much rather use data on daily variation in production, but this information is unavailable.

[23]Indeed, there is evidence that certain air pollutants can have an extended effect on health. For instance, the U.S. Environmental Protection Agency (2006) found that ozone can have an effect on health for up to four days after exposure.

[24]Our multicollinearity tests between $Solar_d$ and $Solar_{d-l}$ for $l = \{1, 2, 3\}$ reveal variance inflation factors (VIFs) of magnitudes close to a 100.

5.2.1 Identifying Assumptions

The validity of our empirical specifications in Equations (1), (2), (3), and (4) relies on, first, the identifying assumption that large-scale investments in solar power generation are exogenous to day-to-day variation in fossil-fuel generation once we control for plant-level characteristics, daily load, demographics, and time fixed-effects. This is a reasonable assumption given that the massive large-scale investments in renewables were encouraged by the ERNC policy, which can be considered a natural experiment (see Section 3.1.1). In this case, variation in solar generation is as good as randomly assigned.

Notwithstanding, the concern of potential endogeneity between power generation and health remains. For instance, power plant locations can be correlated with local income, as local employment and wages may be associated with power plant output. At the same time, higher (lower) wages can correlate with better (worse) health outcomes, and thus, identification of the main parameters in our health equations may be threatened. However, we argue that, by using system-level daily solar generation, we can avoid any localized endogeneity concerns as solar generators are scattered across the entire SING system instead of being concentrated in certain cities (see Figure A4).

However, to guarantee identification, we pair information on average wind direction (see Figure 6) at the power plant level with the results from our displacement analysis, which allows us to distinguish cities downwind of displaced fossil fuel plants.[25] To the extent that large-scale daily solar generation displaces thermal generation, the reduction in emissions from these displaced thermal plants is likely benefiting cities located downwind of these units.[26] Additionally, we identify cities upwind of displaced plants and downwind of non-displaced plants to use later in a robustness analysis. We enrich this wind analysis with the calculation of distances to the displaced thermal plants, and construct an indicator for whether a city is downwind of and near a displaced plant. Thus, when estimating our health equations for all cities, we also do so for cities downwind of displaced fossil fuel plants that are located within $10km$, $50km$, or $100km$ of their boundaries. In doing so, we rely on the identifying assumption that harmful effects of pollution are stronger downwind of and closer

[25] We obtain average wind direction by drawing a pie slice with an angle of $\pi/4$ radians (i.e. 45 degrees) bisected by average daytime wind direction in each location. The resulting average wind direction is: 1.15π radians (206.9 degrees) in Arica (Figure 6(a)), 1.57π radians (282.7 degrees) in Iquique (Figure 6(b)), 1.33π radians (238.6 degrees) in Tocopilla (Figure 6(c)) and 1.09π radians (196 degrees) in Antofagasta (Figure 6(d)).

[26] In the identification of downwind cities, we acknowledge the simplicity of our approach when it comes to understanding how pollution travels over space. However, and to the best of our knowledge, more complex air transport models have not been developed or made public for Chile. This fact reduces our ability to incorporate issues such as the impact of mountain ranges on wind, or wind directions that may change across longer ranges.

to the displaced thermal plants.

6 Results

6.1 Fossil Fuel Displacement

Panel A of Table 3 (Appendix Table A4) presents the results of estimating Equation (1) on the effect of 1-GWh of daily solar generation on daily aggregated generation by fossil fuels (renewable sources). We also include the results of estimating the effect of 1-GWh of daily solar generation on capacity factors in panel B. Columns labeled (2) include stronger time fixed effects than columns labeled (1); further results follow a similar format.

Table 3: The Effect of 1 GWh of Solar Power Generation on Daily Aggregated Fossil Fuel Generation

	Coal		Diesel		Fuel oil		Fuel oil #6		Natural gas	
	(1)	(2)	(1)	(2)	(1)	(2)	(1)	(2)	(1)	(2)
Panel A. Generation (GWh)										
Solar_d	-0.656***	-0.483**	0.151	0.077	-0.011	-0.013	-0.016	-0.014	-0.215	-0.274**
	(0.175)	(0.159)	(0.094)	(0.092)	(0.019)	(0.024)	(0.017)	(0.013)	(0.150)	(0.134)
Panel B. Capacity Factor										
Solar_d	-0.021***	-0.014***	0.015**	0.012	0.047	0.018	-0.018	-0.006	-0.063***	-0.049***
	(0.003)	(0.003)	(0.006)	(0.007)	(0.041)	(0.064)	(0.012)	(0.011)	(0.009)	(0.009)
Obs.	1,915	1,915	1,915	1,915	910	910	1,915	1,915	1,915	1,915
Controls	✓	✓	✓	✓	✓	✓	✓	✓	✓	✓
τ_1 fixed effects	✓		✓		✓		✓		✓	
τ_2 fixed effects		✓		✓		✓		✓		✓

Notes: This table displays estimation results from regressions of daily aggregated fossil fuel generation (panel A) and fossil fuels' daily capacity factors (panel B) on daily solar power generation. Estimation results are marginal effects of daily solar generation (in GWh) derived from an OLS regression on daily aggregated generation, and from a fractional logit response model on daily capacity factors. All estimations include plants with both single- and dual-fuel engines. All regressions include daily temperature, humidity, load and price ratios as controls. Vector τ_1 includes year, month, and weekend fixed effects. Vector τ_2 includes year, seasons, year × seasons, and weekend fixed effects. Bootstrapped standard errors appear in parentheses. Significance levels: $^{*}p < 0.10$, $^{**}p < 0.05$, $^{***}p < 0.001$.

Our findings in Table 3 (and Appendix Table A4) show that solar-generated electricity displaces other fuel sources, particularly dirty sources. From panel A of Table 3, we observe that one additional GWh increase in daily solar generation reduces the day-to-day generation of plants running with coal and with natural gas by 0.48 and 0.27 GWh, respectively (columns 2).[27] Considering the descriptive statistics in Table 1, we observe that this displacement is

[27]Further analysis using simple cycle turbine plants reveals that solar energy displaces coal-fired single-fuel engine generation at a larger magnitude (see Table A5 in the Appendix). This is an indication that the reduced coal use found in Table 3 is attenuated by dual-fuel engine coal-fired plants running with diesel.

roughly equivalent to 1.22% and 5.36% of the daily average electricity generated by these fossil fuels. Indeed, the results for capacity factors in panel B of Table 3 show qualitatively similar results. An extra 1 GWh of solar generation displaces 1.4 percentage points of the capacity factors of plants running with coal, and 4.9 percentage points of the capacity factors of plants running with natural gas. The results in Table 3 also suggest a ramp-up on capacity factors of plants running with diesel. However, this effect disappears once a stronger set of time-fixed effects is included.

The results for renewables in Appendix Table A4 suggest similar displacement effects on hydro, a dispatchable power source. In particular, the results in columns (2) of panel A indicate that, on average, a 1 GWh increase in daily solar generation displaces hydro by 0.007 GWh, equivalent to 3.3% of the average hydro power generated in a single day. Regarding geothermal generation, we find no effects, although the results on capacity factors indicate a statistically significant reduction of four percentage points. While this may be a weak effect, it is important to consider that the geothermal displacement attenuates the potential benefits of a reduction in fossil fuels found in Table 3. Because geothermal energy is a non-emitting source of electricity, its displacement will reduce some of the health benefits associated with the expansion of solar generation. Hydropower, on the other hand, is mostly utilized as a storage resource, dispatching in response to high price times; thus, we are unable to directly identify the environmental impacts of its displacement. Despite this potential attenuation, it is likely that the effect will be minor given the relatively small share of electricity that is produced by hydro and geothermal sources (both of which contribute only 0.4% of mean daily generation; see Table 1). In summary, we expect any attenuation effect from reduced hydro and geothermal generation to be small compared to the benefits of displaced coal and natural gas, which account for 83% and 11% of mean daily generation, respectively.

Finally, we find a positive coefficient of solar generation on wind generation, a non-dispatchable (but curtailable) power source. The result for wind in column (2) of Appendix Table A4 indicates that 1 GWh of daily solar generation ramps up wind generation by 0.099 GWh. Due to the non-dispatchability of wind generation, this likely reflects an underlying correlation of wind and solar, given the thermally driven wind systems that characterize the Atacama Desert (Jacques-Coper et al., 2015). Thermally driven winds are caused by local differences in radiational heating and cooling systems, which in the case of the Atacama favor the complementarity between wind energy and solar energy (Jacques-Coper et al., 2015; Muñoz et al., 2018). An additional source of positive correlation between wind and solar generation may come from the country's effort to boost the adoption of renewable energy sources, which has encouraged the installation of several wind parks in addition to solar power plants (Ministry of Energy, 2013). In any case, given that wind generation is

not dispatchable but is curtailable, the fact that we are not getting a negative coefficient weakly suggests that wind is not curtailed in response to greater solar output, or that, if curtailment exists, it is not large enough to overcome the positive correlation between the two sources.

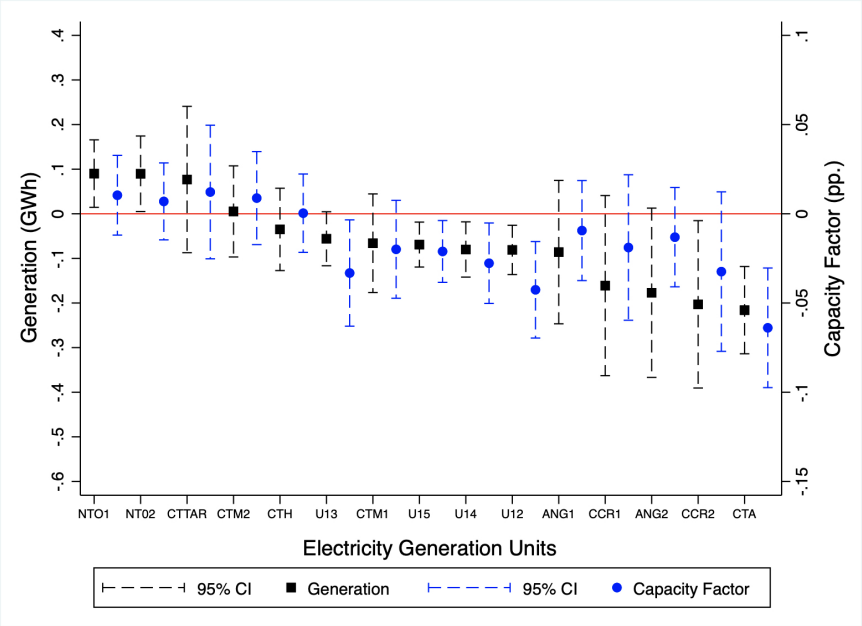

Figure 7: Coal-Fired EGUs and Displacement

Notes: The figure shows estimation results from regressions of daily coal-fired generation (squares) and coal's capacity factors (circles) on daily solar power generation at the electricity generation unit (EGU) level. Point estimates are marginal effects of daily solar generation (in GWh) derived from an OLS regression on daily aggregated generation (left y-axis), and from a fractional logit response model on daily capacity factors (right y-axis). The estimation equations are identical to the ones in columns (2) of Table 3. Dashed lines represent 95% confidence intervals obtained with bootstrapped standard errors. Reference line in red is at the zero mark. All estimations use EGUs that report coal (and its derivatives) as their primary fuel source.

To delve deeper into the displacement of fossil fuel EGUs estimated in Table 3, we estimate Equation (2) on the displacement at the plant level to individually identify the affected plants. We plot the marginal effects of solar generation on daily generation levels and capacity factors by coal-fired EGUs in Figure 7.[28] Squares represent the point estimate of solar generation on daily coal generation (left y-axis), and circles represent the marginal displacement of capacity factors (right y-axis). We observe that the negative impact of solar generation on coal combustion indicated in Table 3 is mostly explained by the shift in the generation of five units: U15, U14, U12, CCR2 and CTA. Figure 7 also reveals the displacement of unit U13, statistically significant at the 10% level. Four of these units

[28]Similar graphs for diesel- and gas-fired units are provided in Appendix Figures A5 and A6, respectively, in the Appendix.

(U15, U14, U13 and U12) are part of the Tocopilla coal-fired power station, which has been in operation since 1960 and is SING's oldest coal-fired plant.[29] The largest generation displacement is found for the CTA unit that belongs to the Atacama station. Power output for this unit decreased by 216 MWh, roughly equivalent to 7% of its capacity. Considering this plant alone, this displacement translates into more than 200 MWh of avoided daily coal-fired generation. This is closely followed by reductions in CCR2's output, one of the largest EGUs in the system (274.9 MW of gross capacity).[30] On average, our estimates reveal that 1 GWh of solar generation displaces 203 MWh of generation from the Atacama plant on a given day.

In addition to the displacement of several coal-fired units, Figure 7 also reveals a statistically significant ramp-up in the power generation of two facilities: NTO1 and NTO2. On average, 1 GWh of daily solar generation increases generation in these plants by 90 and 89 MWh, respectively, jointly equivalent to 0.46% of the daily coal-fired generation (see Table 1). These two units are part of the Norgener power plant, also located in Tocopilla. Although the ramp-up in the generation of these two coal-fired units is significantly lower than the displacement found at other facilities, the increase slightly attenuates the potential health impact of the overall set of displaced plants in Tocopilla.

6.2 Solar Generation and Health Outcomes

The results on the effect of 1 additional GWh of solar generation on the rate of daily hospital admissions using Equation (3) are displayed in Table 4 for cardiovascular (panel A) and respiratory (panel B) conditions, including the detail between upper (panel C) and lower (panel D) respiratory diseases. We present these results using alternative subsamples of downwind cities as defined in Section 5. Columns (1) and (2) both include controls that capture time variation (year, seasons, year $\times$ seasons, and weekend fixed effects), weather conditions, and city-level demographics and mining production.[31] In addition, columns (1) include city fixed effects, while columns (2) include city $\times$ year fixed effects. This last column is our preferred specification.

Altogether, the results in Table 4 indicate that solar generation leads to a reduction in hospital admissions. The results for our preferred specification (columns (2)) show that, across all cities, 1 GWh increase in solar generation leads to a 6.7 percent reduction in the rate of daily admissions due to all respiratory conditions (panel B), with the majority of

[29] At the time of writing, the Chilean government announced its plans to shut down these four units between 2019 and 2024. Source: Online. Retrieved: December 2019.

[30] Units CCR1 and CCR2 belong to the Cochrane Power Station, with more than 500 MW of gross capacity.

[31] It is important to control for mining production as this sector is a significant polluter in the area and the largest buyer of SING's power. See Section 5 for more details.

Table 4: The Effect of Daily Solar Generation on the Daily Rate of Hospital Admissions

	All Cities		Cities Downwind of Displaced Fossil Fuel Plants					
			$< 10km$		$< 50km$		$< 100km$	
	(1)	(2)	(1)	(2)	(1)	(2)	(1)	(2)
Panel A. Cardiovascular								
Solar_d	-0.028*	-0.023	-0.056	-0.046	-0.038	-0.037	-0.032	-0.030
	(0.016)	(0.014)	(0.052)	(0.062)	(0.039)	(0.037)	(0.027)	(0.022)
Panel B. All respiratory								
Solar_d	-0.067***	-0.067***	-0.133**	-0.106**	-0.094**	-0.090**	-0.058**	-0.045*
	(0.016)	(0.015)	(0.049)	(0.049)	(0.035)	(0.035)	(0.023)	(0.024)
Panel C. Upper respiratory								
Solar_d	-0.028**	-0.027	-0.024***	-0.024***	-0.015***	-0.014**	-0.014***	-0.018***
	(0.009)	(0.025)	(0.002)	(0.003)	(0.003)	(0.005)	(0.003)	(0.002)
Panel D. Lower respiratory								
Solar_d	-0.038***	-0.037***	-0.123***	-0.117*	-0.082	-0.079*	-0.067***	-0.066***
	(0.009)	(0.008)	(0.035)	(0.064)	(0.149)	(0.043)	(0.017)	(0.018)
Obs.	36,385	36,385	3,830	3,830	5,745	5,745	7,660	7,660
Number of Cities	19	19	2	2	3	3	4	4
Controls	✓	✓	✓	✓	✓	✓	✓	✓
City fixed effects	✓		✓		✓		✓	
City×Year fixed effects		✓		✓		✓		✓

Notes: This table displays estimation results from regressions of daily hospital admissions on daily solar power generation. Solar generation is in GWh. Estimation results are marginal effects from ZINB regressions offsetting by population. Controls include weather, mining production, and demographic covariates. All regressions include controls, year, seasons, year × seasons, and weekend fixed effects in both the main and the inflate equations. Clustered standard errors by city appear in parentheses. Significance levels: $^{*}p < 0.10$, $^{**}p < 0.05$, $^{***}p < 0.001$.

this reduction coming from lower respiratory hospitalizations (roughly 55%). Results for cardiovascular (panel A) and upper respiratory (panel C) hospitalizations are also negative but statistically insignificant at the conventional levels. Although these results have the expected sign, they could be underestimating the true health effect of solar power generation if emissions from displaced fossil fuel plants are not equally distributed across space. Thus, to better understand the effect of solar on health through the displacement of emissions from dirty generators, we redefine our sample to include cities located downwind of and at different distances from displaced fossil fuel plants. We present these results in the last six columns of Table 4.

With this subsample, we obtain a stronger and larger effect on the rate of admissions due to respiratory conditions near displaced plants ($< 10km$), although the coefficients on cardiovascular conditions continue to lack statistical significance. For cities within $10km$ downwind of displaced plants, the results in column (2) indicate that a 1-GWh increase in daily solar generation results in a 10.6 percent reduction in hospital admissions due to all respiratory diseases. These reductions are statistically significant for admissions due to both

upper and lower respiratory conditions, although the latter are larger in magnitude. The signs and statistical significance of the estimated effects are slightly similar for cities within $50km$ and within $100km$ of distance from the displaced facilities, albeit with decreasing magnitudes. For instance, the 10.6 percent reduction in admissions due to all respiratory diseases found within $10km$ of displaced thermal plants, decreases to 9 percent within $50km$ and to 4.5 percent within $100km$. This decay is consistent with the identifying assumption that the health benefits from thermal generation displacement decrease with distance from the displaced sources. Overall, the results in Table 4 suggest that solar power generation leads to better health outcomes likely attributable to improvements in local air quality.

We repeat the exercise in Table 4 by estimating Equation (3) across different age groups. We present these results in Figure 8 for all cities using our preferred specification. Full estimation results are given in Appendix Tables A6, A7, A8, and A9, for all cities, and for cities downwind $10km$, downwind $50km$, and downwind $100km$, respectively.

The results in Figure 8 show that additional solar power generation leads to health benefits across most age groups in our sample of all cities, particularly the most vulnerable groups (infants, toddlers, kids, and seniors). Figure 8(a) shows that one additional GWh of solar power generation reduces cardiovascular-related hospital admissions of kids by .27%. We also observe a negative effect among adults and seniors, but we lose some precision in the estimation of these coefficients. Figure 8(b) indicates a clear reduction in hospital admissions of infants and seniors by 2% and 1.1%, respectively (see Appendix Table A6). Similarly, the estimated marginal effects for upper respiratory diseases in panel 8(c) show statistically significant reductions in hospital admissions of kids (1.1%) and seniors (.13%), while panel 8(d) on lower respiratory diseases show similar and stronger morbidity effects among infants (2.1%), toddlers (1.5%), and seniors (.9%).

Moving to our preferred subsample of cities (those near and downwind to displaced fossil fuel plants) in Tables A7, A8, and A9, shows that the sign of the estimated coefficients is preserved, yet due to the reduction in the number of observations, the power of our estimations is restricted and the statistical significance reduced in some cases. For instance, we obtain a negative effect among kids and hospital admissions due to cardiovascular diseases, but these effects are statistically insignificant. Notwithstanding, we observe statistically significant reductions in admissions due to all respiratory diseases among infants and seniors. In this case, we observe a 5.3% reduction in hospital admissions of infants in downwind cities within $10km$ of displaced plants (Appendix Table A7). This effect decreases to a 3.5% reduction in downwind cities within $50km$ (Appendix Table A8), and to a 2.7% in downwind cities within $100km$ (Appendix Table A9). We find similar effects for seniors, and among kids and seniors when it comes to admissions due to lower respiratory diseases, although

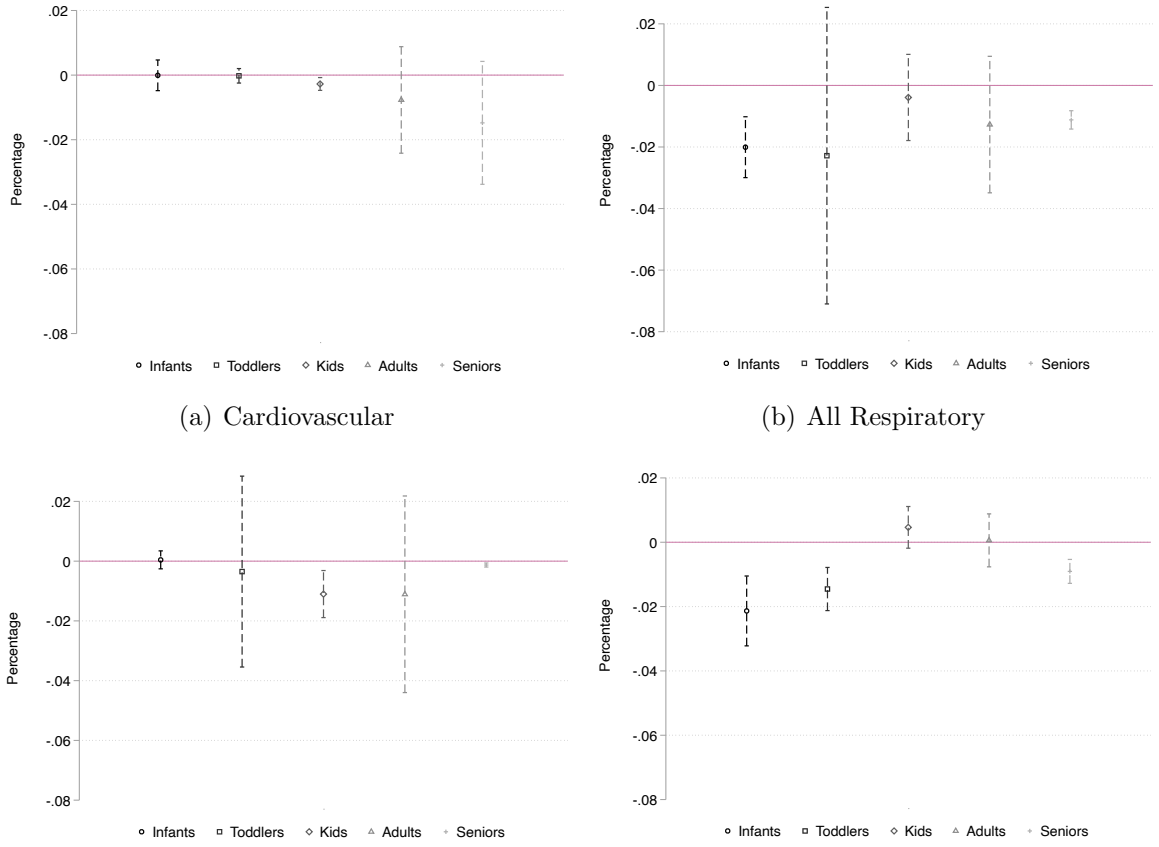

(a) Cardiovascular

(b) All Respiratory

(c) Upper Respiratory

(d) Lower Respiratory

Figure 8: The Effect of Daily Solar Generation on the Daily Rate of Hospital Admissions by Age Group – All Cities

Notes: This figure plots estimation results from regressions of daily hospital admissions on daily solar power generation across all cities by age group. Solar generation is in GWh. Estimation results are marginal effects from ZINB regressions offsetting by population. All regressions include controls (weather, mining production, and demographics), year, seasons, year × seasons, and weekend fixed effects in both the main and the inflate equations. Dashed lines are 95% confidence intervals obtained with clustered standard errors by city.

they are less precise. The results obtained for all respiratory diseases, however, confirm the health benefits of increased solar power generation among vulnerable groups such as infants and seniors, which become stronger in cities downwind of and in close proximity to displaced thermal plants.

6.2.1 Short- Versus Long-Term Health Effects

The results in Table 4 and Figure 8 offer a general perspective of the net effect that day-to-day variation in solar generation has on day-to-day variation in hospital admissions, suggesting the existence of short-term benefits of additional solar generation on health.

Additional evidence of the immediate co-benefit of solar is found in the results for infants in panels (b) and (d) of Figure 8 (equivalent to panels B and D in Table A6). As stated in Currie and Neidell (2005), the link between cause and effect is immediate in the case of infants, whereas diseases today in adults, for instance, may reflect pollution exposure from years ago. The negative and statistically significant effects of solar generation on hospital admissions of infants due to respiratory diseases, particularly lower respiratory diseases, found in panels B and D of Table A6 illustrate this immediate link. Comparable effects are found in panel B of Tables A7, A8, and A9. Considering that infants are less than one year old, these findings corroborate the contemporaneous aspect of the co-benefits of solar power generation.

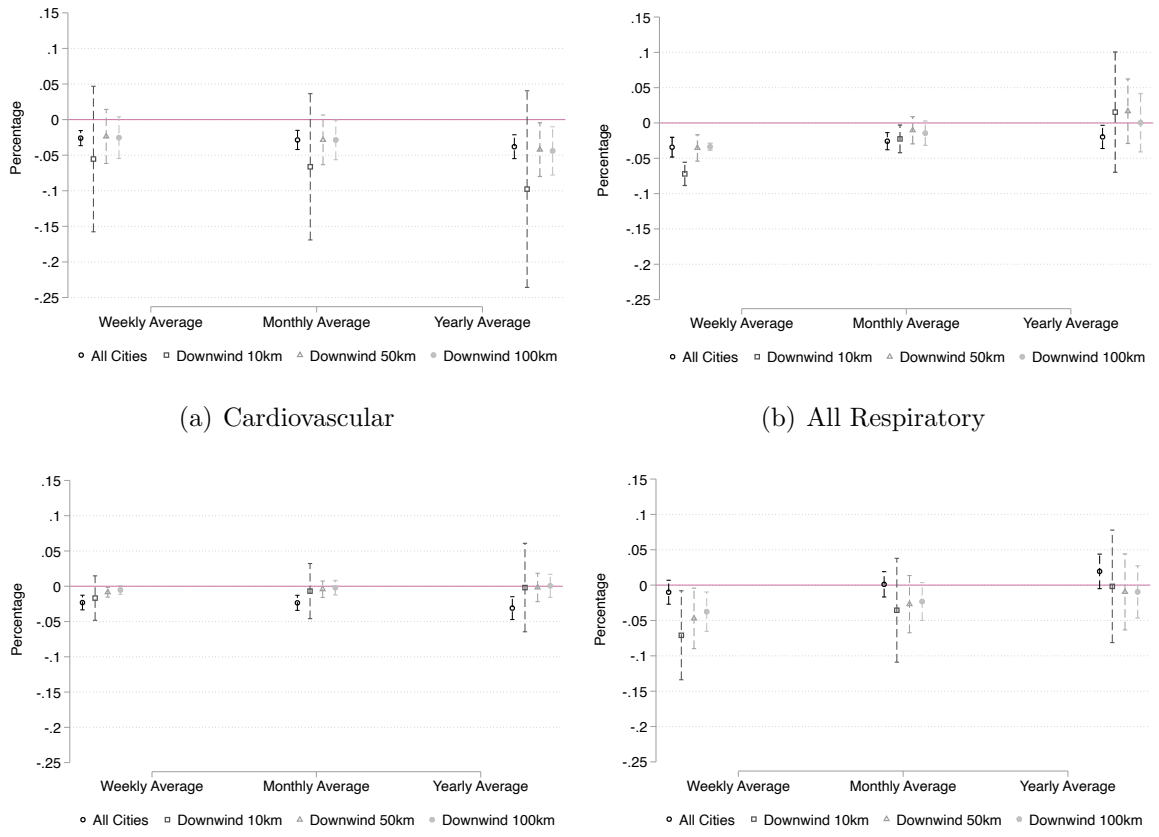

(a) Cardiovascular

(b) All Respiratory

(c) Upper Respiratory

(d) Lower Respiratory

Figure 9: The Long-Term Effect of Average Solar Generation on the Daily Rate of Hospital Admissions

Notes: This figure shows estimation results from regressions of daily hospital admissions on weekly, monthly, and yearly average solar power generation. Solar generation is in GWh. Point estimates are average partial effects from ZINB regressions using 300 iterations and offsetting by population. All regressions include controls (weather, mining production, and demographics), year, seasons, year × seasons, and weekend fixed effects in both the main and the inflate equations. Dashed lines are 95% confidence intervals obtained by clustering standard errors by city.

As an additional test on whether these co-benefits are masking some permanent effects, we estimate Equation (4) where the main explanatory variable is allowed to reflect the moving weekly, monthly or yearly average solar generation in the system. Equation (4) also allows us to take into account potential lagged effects of solar generation on contemporaneous health outcomes, albeit indirectly. To that end, we replace S_d by S_t, where $t = \{w, m, y\}$. Modeled in this way, δ_t gives us the average marginal effect of 1 GWh of either weekly, monthly or yearly average solar generation on the rate of daily relevant hospitalizations. The results using our strongest specification are displayed in Figure 9, with point estimates and corresponding standard errors shown in Appendix Table A10. Appendix Table A11 contains similar results using weekly, monthly, and yearly maximum solar generation.

The results in Figure 9 show larger reductions in hospitalizations from weekly average generation relative to the contemporaneous results shown in columns (2) of Table 4, particularly for cities downwind of nearby fossil fuel plants ($< 10km$). The fact that this coefficient is slightly greater than the daily impact as reported in Table 4 suggests an additional effect of reduced cumulative pollution exposure. However, these cumulative effects seem to be present only in the relatively short term, as they become smaller and generally less significant as we move toward longer times of exposure (monthly and yearly). We take these estimates together with our previous results among infants as compelling evidence of the immediate health effects of increased solar power generation.

6.2.2 Solar, Fossil Fuels, Pollution, and Health

Our previous health results systematically indicate significant reductions in air pollution-related hospitalizations due to variation in solar power generation. These reductions are found mostly in cities downwind of fossil fuel plants that are displaced by solar generation as revealed by our plant-level displacement analysis (see Section 6.1). This strategy helps us to incorporate the air transport of pollutants emitted by the displaced thermal plants, but it constitutes an indirect test of the mechanism through which solar generation affects health. In this section, we employ a more direct test on the channel through which solar power generation is positively affecting pollution-related morbidity by using available data on $PM_{2.5}$ concentrations. As mentioned in Section 3.1.2, pollution data in Chile is scarce for cities other than Santiago. However, we gathered publicly available daily $PM_{2.5}$ records for some of the cities hosting fossil fuel generators, and some which are downwind of displaced fossil fuel plants.[32] We use these data to first explore the link between thermal generation and

[32]Specifically, we have data for Arica, Antofagasta, Tocopilla and Alto Hospicio. The last two cities, namely Tocopilla and Alto Hospicio, are part of the group of cities within $10km$ downwind of displaced fossil fuel plants. Data are daily records averaged across stations from 2012 to 2017, and come from the National

air pollution concentrations by estimating the effect of daily fossil fuel generation (i.e., coal, diesel, and natural gas) on city j's daily $PM_{2.5}$ concentrations (in logs). To avoid endogeneity concerns, we use total fossil generation across these four cities instead of city-level generation as follows:

$$\log(PM_{2.5})_{jd} = \rho_0 + \rho_1 Coal_d + \rho_2 Diesel_d + \rho_3 NaturalGas_d + \beta Load_{jd} + \omega_{jd} + \zeta + \tau + \upsilon_{jd}, \quad (5)$$

where j indexes cities and d indexes days. The variable $Load_{jd}$ represents j's daily electricity demand that also works as a proxy for j's daily economic activity.[33] The vector ω_{jd} considers daily city-level weather covariates (including wind speed, also available for these cities); ζ is a vector of demographics, mining production and city times year fixed effects; τ is a vector of time-fixed effects; and υ_{jd} is an idiosyncratic error. In an alternative specification, we replace city j's daily thermal power generation for the system-level daily solar generation ($Solar_d$). We estimate Equation (5) with an OLS estimator using Newey–West standard errors to control for potential autocorrelation known to affect the pollution data. We present these results in Table 5 using city fixed effects (columns (1) and (3)) and city $\times$ year fixed effects (columns (2) and (4)).

The results from our preferred specification (column (2)) in Table 5 show that, on average, 1-GWh increase in diesel-fired generation increases $PM_{2.5}$ concentrations by 13%, while a 1-GWh increase in gas-fired generation increases $PM_{2.5}$ by 1.3% across the subsample of cities hosting fossil fuel generation. Recall that all gas-fired plants in our sample are combined-cycled plants that operate also using diesel, so this effect is likely due to the use of diesel in gas-fired plants. We do not observe a statistically significant effect of coal-fired generation across all cities. However, when selecting cities downwind of displaced plants, we obtain that a 1-GWh increase in coal-fired generation increases $PM_{2.5}$ concentrations by 1.4% (column (2), downwind cities). One additional GWh of diesel-fired generation is related to a 10.8% increase in fine PM concentrations, while additional gas-fired generation is found to increase these concentrations by 1.5% within these cities. Considering that daily concentrations of this pollutant are roughly 17.49 $\mu g/m^3$, on average, in cities downwind $10km$ (see Appendix Table A12), one extra GWh of coal, diesel, and natural gas combustion is equivalent to an additional concentration of 0.245, 1.889, and 0.262 $\mu g/m^3$, respectively, of daily $PM_{2.5}$ concentrations during the period of solar installations.

Next, we include solar generation in the estimation of Equation (5) in two ways. First,

Air Quality Information System (SINCA)'s website, https://sinca.mma.gob.cl. Descriptive statistics for this variable are in Appendix Table A12.

[33] Our load data are at the system level. Thus, to approximate city-level load, we first calculate a per-capita load given total population across the four cities. Then, we multiply this per-capita load by the population of the city, producing an approximation of city-level load.

Table 5: The Effect of Daily Power Generation on Daily $PM_{2.5}$

	All Cities With Fossil Fuel Plants				Cities $< 10km$ Downwind of Displaced Fossil Fuel Plants			
	(1)	(2)	(3)	(4)	(1)	(2)	(3)	(4)
$Coal_d$	0.004	0.004		0.003	0.014**	0.014**		0.013**
	(0.003)	(0.003)		(0.003)	(0.005)	(0.005)		(0.005)
$Diesel_d$	0.130**	0.130**		0.120**	0.108*	0.108*		0.093
	(0.048)	(0.046)		(0.047)	(0.062)	(0.062)		(0.061)
Natural Gas_d	0.013***	0.013***		0.013***	0.015**	0.015**		0.016**
	(0.004)	(0.004)		(0.004)	(0.005)	(0.005)		(0.006)
$Solar_d$			-0.033**	-0.027**			-0.043**	-0.033*
			(0.013)	(0.013)			(0.019)	(0.019)
Obs.	5,582	5,582	5,319	5,319	2,592	2,592	2,329	2,329
Number of Cities	4	4	4	4	2	2	2	2
City fixed effects	✓		✓		✓		✓	
City×Year fixed effects		✓		✓		✓		✓

Notes: This table displays estimation results from regressions of daily average fine particle matter ($PM_{2.5}$) concentrations (in logs) on daily fossil-fueled power generation and on daily system-level solar generation. Power generation is in GWh. Estimation results are marginal effects from OLS regressions using Newey–West standard errors (in parentheses) allowing for up to three lags in the dependent variable. All regressions include weather controls (minimum and maximum temperature, humidity, wind speed), mining production, demographic covariates (including population), city-level load, year, seasons, year × seasons, and weekend fixed effects. Significance levels: $^{*}p < 0.10$, $^{**}p < 0.05$, $^{***}p < 0.001$.

we do so by replacing thermal generation with solar generation as a regressor (results in columns (3) of Table 5), and second, we include it as an additional regressor (results in columns (4) of Table 5). In both cases, we find negative and significant results for solar generation. Namely, the results in columns (4) of Table 5 indicate that 1 extra GWh of solar generation reduces $PM_{2.5}$ concentrations by 3–4% across the two different groups of cities. Altogether, the findings in Table 5 indicate that thermal generation effectively increases airborne pollution concentrations, while solar generation has the opposite effect.

Our final exercise considers the information in Table 5 in tandem with our health analysis by means of two different approaches. First, we re-estimate our baseline health equations but replace solar generation with city-level daily average $PM_{2.5}$ concentrations in order to estimate the direct effect of pollution concentrations on our morbidity outcomes. In doing this, we have to consider the potential endogeneity in this specification. For instance, $PM_{2.5}$ can be formed due to chemical reactions of secondary particles from SO_2 and NO_X, pollutants that are common to coal combustion and also have a direct impact on health (World Health Organization, 2006). In addition, other factors such as economic conditions may have a simultaneous impact on both health outcomes and air pollution concentrations. Thus, while informative, omitted factors in this regression may give us an inconsistent estimator of the

pollution impact on health. We present the results of this first approach in columns (1) of Table 6. For robustness, we also present the results of this regression using a Poisson estimator in columns (2).

Table 6: The Effect of Daily $PM_{2.5}$ on the Daily Rate of Hospital Admissions

	All Cities				Cities $< 10km$ Downwind of Displaced Fossil Fuel Plants			
	(1)	(2)	(3)	(4)	(1)	(2)	(3)	(4)
Panel A. Cardiovascular								
$PM_{2.5}$	0.008	0.010*	0.010	0.005	-0.0003	0.001*	-0.002	0.026
	(0.006)	(0.005)	(0.006)	(0.014)	(0.0003)	(0.0003)	(0.001)	(0.035)
$PM_{2.5} \times Solar_d$			0.0004				0.001	
			(0.002)				(0.002)	
$\hat{\rho}$				-0.004				-0.028
				(0.014)				(0.036)
Panel B. All respiratory								
$PM_{2.5}$	0.060***	0.043***	0.051***	0.075***	0.018***	0.018***	0.024***	0.097***
	(0.015)	(0.005)	(0.006)	(0.015)	(0.003)	(0.004)	(0.003)	(0.026)
$PM_{2.5} \times Solar_d$			-0.010**				-0.007***	
			(0.005)				(0.002)	
$\hat{\rho}$				-0.061***				-0.083***
				(0.014)				(0.024)
Panel C. Upper respiratory								
$PM_{2.5}$	0.002	0.001	0.003	0.134**	0.004	0.004**	0.005***	0.239***
	(0.008)	(0.005)	(0.005)	(0.049)	(0.002)	(0.001)	(0.001)	(0.024)
$PM_{2.5} \times Solar_d$			-0.004**				-0.002***	
			(0.002)				(0.000002)	
$\hat{\rho}$				-0.124**				-0.224***
				(0.045)				(0.036)
Panel D. Lower respiratory								
$PM_{2.5}$	0.037**	0.038***	0.043***	0.075***	0.015***	0.014**	0.018***	0.088**
	(0.011)	(0.011)	(0.009)	(0.015)	(0.003)	(0.006)	(0.005)	(0.028)
$PM_{2.5} \times Solar_d$			-0.005*				-0.003**	
			(0.003)				(0.001)	
$\hat{\rho}$				-0.056***				-0.073**
				(0.014)				(0.024)
Obs.	5,582	5,582	5,319	5,319	2,592	2,592	2,329	2,329
Estimation	ZINB	Poisson	Poisson	IV-Poisson	ZINB	Poisson	Poisson	IV-Poisson
Number of Cities	4	4	4	4	2	2	2	2
City×Year fixed effects	✓	✓	✓	✓	✓	✓	✓	✓

Notes: This table displays estimation results from regressions of daily hospital admissions by disease on daily average $PM_{2.5}$ concentrations. Estimation results are marginal effects from ZINB, Poisson, and IV-Poisson estimations using daily solar generation as an instrument for $PM_{2.5}$ and offsetting by population. Daily $PM_{2.5}$ are measured in $\mu g/m^3$. Solar generation is in GWh. The IV-Poisson estimation uses a GMM Control Function estimator, where the parameter ρ measures the strength of the endogeneity of $PM_{2.5}$. All regressions include weather controls (minimum and maximum temperature, humidity, wind speed), mining production, demographic covariates, year and weekend fixed effects. Due to lack of convergence, we remove seasons and year × seasons fixed effects. Clustered standard errors by city appear in parentheses. Significance levels: $^{*}p < 0.10$, $^{**}p < 0.05$, $^{***}p < 0.001$.

The results in columns (1) and (2) of Table 6 suggest that additional $PM_{2.5}$ concentrations increase morbidity, particularly those associated with respiratory diseases. We also find a positive effect on cardiovascular outcomes, but they are very small and only borderline

significant. To test how this effect changes with solar generation, we include the interaction between $PM_{2.5}$ and $Solar_d$ in column (3) as an additional regressor. As expected, additional concentrations of $PM_{2.5}$ continue to negatively affect health. Yet this effect decreases with more GWhs of solar generation in the grid, as shown by the negative estimate for the interacting term. These findings support our results related to the direct impact of solar on health, namely, more solar and less fossil fuel generation reduce emissions and in turn, hospitalizations. Furthermore, the fact that we do not find a direct effect of pollution on cardiovascular hospitalizations explains our lack of significance on cardiovascular hospitalizations in our main specification.

Although promising, these results are likely endogenous. To deal with the potential endogeneity of $PM_{2.5}$, we replicate the exercises in columns (2) but use day-to-day variation in solar generation as an instrument for $PM_{2.5}$. Due to the nature of our outcome variable (a count variable), we estimate this with a Poisson Instrumental Variable approach that uses a Control Function (CF) estimator (Wooldridge, 2010) with a Generalized Method of Moments (GMM) procedure.[34] In a CF procedure, the residuals $\hat{v}$ derived from the regression of $PM_{2.5}$ on $Solar_d$ are included in the main estimation equation to control for the endogeneity of $PM_{2.5}$. A statistically significant estimate for the coefficient on $\hat{v}$ constitutes a simple test on the endogeneity of $PM_{2.5}$ (Wooldridge, 2010). We present these results in columns (4) of Table 6, including the estimated coefficient of the CF residuals, $\hat{\rho}$.

The statistical significance of $\hat{\rho}$ in Table 6 tells us that $PM_{2.5}$ is indeed endogenous in the regressions that use the rate of hospital admissions due to respiratory diseases as outcomes. Moreover, instrumenting $PM_{2.5}$ results in larger coefficients relative to those that do not consider the endogeneity of pollution, which shows the downward bias of the estimates in column (2). At the same time, these larger-in-magnitude estimates signal that the use of day-to-day variation in solar generation allows us to effectively capture variation in hospital admissions due to changes in daily $PM_{2.5}$ concentrations in full. We take the results in Tables 5 and 6 as strong evidence that the co-benefits of solar power generation on hospital admissions found throughout our analysis are largely due to reductions in local airborne pollution from displaced thermal generation.

[34] We do this with the *IVPOISSON* command in Stata®, which allows us to derive correct standard errors through the application of GMM in one single stage.

7 Robustness Checks

7.1 Alternative Groups of Cities

Our results are robust to several alternative specifications. First, we check the robustness of our wind direction analysis by using cities with fossil fuel plants as an approximation to cities with pollution exposure. From our displacement analysis, we are also able to consider: 1) cities upwind of displaced plants, 2) cities downwind of non-displaced plants, and 3) cities downwind of ramping-up plants (see Figure 7). This latter group, however, is quite restrictive as it ultimately limits the cities to just one. We present these results in Table 7.

Table 7: The Effect of Daily Solar Generation on the Daily Rate of Hospital Admissions Using Alternative Groups of Cities

	With Fossil Fuel Generation		Upwind of Displaced Plants		Downwind of Non-displaced Plants		Downwind of Ramping-Up Plants	
	(1)	(2)	(1)	(2)	(1)	(2)	(1)	(2)
Panel A. Cardiovascular								
Solar_d	-0.066	-0.077	-0.001	-0.001	-0.0002	-0.003	0.063	-0.049
	(0.051)	(0.054)	(0.001)	(0.002)	(0.002)	(0.004)	(0.103)	(0.098)
Panel B. All respiratory								
Solar_d	-0.206***	-0.218***	-0.002	-0.002	0.001	0.001	0.293**	-0.127
	(0.047)	(0.044)	(0.003)	(0.004)	(0.003)	(0.003)	(0.123)	(0.143)
Panel C. Upper respiratory								
Solar_d	-0.094***	-0.095***	-0.0003	-0.0001	0.0003	0.0003	0.042	-0.039
	(0.015)	(0.015)	(0.094)	(0.005)	(0.001)	(0.019)	(0.082)	(0.086)
Panel D. Lower respiratory								
Solar_d	-0.113***	-0.126***	-0.001	-0.002	0.003***	0.001	0.236**	-0.097
	(0.031)	(0.031)	(0.002)	(0.004)	(0.0003)	(0.001)	(0.085)	(0.098)
Obs.	9,575	9,575	11,490	11,490	5,745	5,745	1,915	1,915
Number of Cities	5	5	6	6	3	3	1	1
τ_1 fixed effects							✓	
τ_2 fixed effects	✓	✓	✓	✓	✓	✓		✓
City fixed effects	✓		✓		✓			
City × Year fixed effects		✓		✓		✓		

Notes: This table displays estimation results from regressions of daily hospital admissions on daily solar power generation using alternative cities. Solar generation is in GWh. Estimation results are marginal effects from ZINB regressions offsetting by population. All regressions include controls (weather, mining production, and demographics) in both the main and the inflate equations. Vector τ_1 includes year, month, and weekend fixed effects. Vector τ_2 includes year, seasons, year × seasons, and weekend fixed effects. Clustered standard errors by city appear in parentheses for all group of cities except for cities downwind ramping-up plants that use robust standard errors. Significance levels: $^{*}p < 0.10$, $^{**}p < 0.05$, $^{***}p < 0.001$.

Splitting the sample in this manner reveals that reductions in hospitalizations attributable to solar generation are primarily found in places with fossil fuel generation. The results in the first two columns of Table 7 suggest that additional solar generation predominantly curtails

respiratory admissions in cities where displacement is possible. Namely, an additional 1 GWh of solar generation results in a 21.8 percent reduction of all respiratory hospitalizations in cities that house fossil fuel plants, of which the majority of these effects are reductions in lower respiratory hospitalizations. Similar to our findings with all cities and downwind cities, we do not find a statistically significant impact on cardiovascular-related hospitalizations.

We also find that cities that are upwind of displaced plants or downwind of non-displaced plants are not generally affected by solar, as almost all coefficients are statistically insignificant and very small. The one exception is with lower respiratory hospitalizations, in which we find a small and positive effect of solar on hospitalizations in cities downwind of non-displaced plants. However, this effect goes away with our preferred fixed effects specification. These results provide another proof of our identification strategy holding, as controlling for wind direction allows us to more accurately identify the impact of solar on health.

Finally, we find large positive effects of solar on lower respiratory hospitalizations in cities that are downwind of plants that have ramped up in response to solar generation (column (1)). Our plant-level analysis shows that two coal-fired plants and one gas-fired unit ramp up their production in response to the injection of this renewable (see Figure 7 and Appendix Figure A6). Thus, it is not surprising that respiratory hospitalizations increase in this subsample. Yet this effect disappears once we utilize our preferred set of time-fixed effects.

7.2 Alternative Estimation Methods

We also test the robustness of our ZINB estimation method by utilizing alternative estimators: a Poisson estimator, an OLS, and a Negative Binomial. Unlike ZINB, the Poisson estimator does not take into account the overdispersion in the data, and neither the Negative Binomial estimator nor OLS consider the zero-inflation of the outcomes (the pile-up at zero). The results are displayed in Appendix Tables A13, A14, and A15, respectively.

Our Poisson results in Appendix Table A13 are very similar to the results obtained by utilizing ZINB: specifically, we find that a 1 GWh increase in solar generation reduces all respiratory hospitalizations by 6.7 percent in all cities, and 14.4 percent in nearby downwind cities. Similar to the ZINB results, we also find that the effect is largest in downwind cities at distances closest to the displaced plant, with effect sizes reducing at further distances. Again, we do not find a statistically significant effect for cardiovascular hospitalizations in this specification.

Regarding OLS, the results in Appendix Table A14 show similar magnitudes of reduced hospitalizations across all cities, although we lose significance when subsampling to downwind cities alone. In order to use this estimator, we change our outcome variable from a discrete

to continuous form by dividing hospital admissions by population (measured in 100,000). However, it's important to point out that OLS is not a methodology that accurately deals with a dependent variable that has an abundance of observations with zero values (pile-up at zero). Thus, though the OLS results in Table A14 are useful as a first approximation, we take them with caution given the skewed distribution of the dependent variable.

Finally, the results in Appendix Table A15 for the Negative Binomial show similar reductions in respiratory hospitalizations as the ZINB results, with 1 GWh of solar reducing all respiratory hospitalizations by 6.8 percent in all cities and by 14.3 percent in downwind cities. These findings demonstrate that our results are robust to the choice of estimator.

7.3 Placebo Health Outcomes

Additionally, we test whether solar generation affects health outcomes that are, presumably, unrelated to pollution. Appendix Table A16 displays the ZINB results of this falsification test using infections (panel A) and blood diseases (excluding anemia) (panel B). We also include Schlenker and Walker (2016)'s placebo outcomes: strokes (panel C), bone fractures (panel D) and appendicitis (panel E).[35] The placebo results are all small and statistically insignificant, regardless of the group of cities considered, except for appendicitis. For admissions related to this disease, we find that they decrease with solar across all cities but increase across cities further than $10km$ downwind of displaced plants. However, this positive effect disappears once we consider our preferred specification in column (2). Whether this result is due to peculiar dynamics derived from hospital capacity constraints commonly experienced by developing countries (Guidetti et al., 2021) remains an open avenue for future research.

8 Discussion

The remarkable and rapid expansion of solar generation capacity in Chile has provided a natural experiment to test the impact of renewable electricity sources on morbidity in a developing country. We run a variety of different tests to quantify the health benefits of almost 600 MW of new solar generation capacity. Overall, our results tell a positive story about how we can employ solar energy to bring about improved health outcomes in settings with elevated pollution exposure and reduced healthcare access.

[35] The exact ICD-10 codes are A00/A099, A200/A799 and B50/B999 for infections (we exclude tuberculosis A15/A19 and viral infections B00/B499); D65/D899 for blood disorders (excluding anemia); I60/I699 for strokes; S000/S999 for bone fractures; and K350/K389 for appendicitis.

We first demonstrate that solar energy can effectively displace fossil fuel plants, notably plants that rely on coal and natural gas. These heavy emitters are displaced by increases in solar generation, although the benefits may be attenuated by the ramp-up of a subset of fossil fuel generators and the reductions in hydro and geothermal electricity. However, given the relatively small shares of these fuel types in generation, the attenuation of displacement is not enough to offset the positive health benefits.

We next show that the day-to-day operation of solar plants reduces daily hospitalizations of cardiovascular and respiratory diseases, particularly those related to the upper airways. When taking into account the transport of pollutants using cities downwind of fossil fuel plants displaced by solar generation, we find significant morbidity reductions associated with all types of respiratory diseases, noticeable up to $50km$ from the displaced facilities, and up to $100km$ in the case of lower respiratory diseases (though the effect size is largest for towns closest to the displaced plants). Across different age groups, we find the largest statistically significant impacts on hospitalizations of infants, children and seniors, the most vulnerable age groups. A simple linear projection of our results suggests that a full solar displacement of all coal-fired generation in the current grid would imply, in cities downwind of displaced thermal plants, 762 and 214 fewer respiratory admissions of infants and seniors per year, respectively. In the case of toddlers and kids, a full solar displacement would imply a reduction of 470 and 55 lower respiratory admissions in cities downwind of displaced thermal plants.[36] Furthermore, we show that the health co-benefits of solar generation are strongest in the short-term, and in cities downwind of displaced plants or those hosting fossil fuel generation. This latter result demonstrates the geographic heterogeneous effect of solar generation, and simultaneously suggests that areas with intense fossil fuel generation will benefit more from an expansion of renewable, clean energy sources.

Our results remain unaltered after using several robustness checks, which include the use of cities without thermal generation, upwind cities, cities downwind of nondisplaced plants, and cities downwind of plants that have ramped up. Our results are also robust to alternative estimation approaches, including utilizing Poisson, OLS, and negative binomial models, and to the use of hospital admissions due to other conditions presumably not related to pollution. We do find a significant decrease in appendicitis admissions across all cities. However, this result disappears once we use our preferred specification across cities downwind of displaced plants. A plausible explanation for this unexpected result across all cities is a rearrangement of admissions due to the temporary alleviation of otherwise strained hospitals—a common

[36] Values are taken from the age-specific coefficients in Table A7, columns (2), statistically significant results only. Infants: -0.0531 × 39.36 GWh (average daily coal-fired generation) × 365 = 762. Toddlers: -0.0327 × 39.36 GWh × 365 = 470. Kids: -.0038 × 39.36 GWh × 365 =55. Seniors: -0.0149 × 39.36 GWh × 365 = 214.

characteristic in developing countries. However, this explanation would require further research, which is outside the scope of this project.

Our study provides important evidence that solar generation can bring about positive health outcomes in developing nations, increasing the social benefits of investment in power generation capacity for these clean resources. To the extent that these countries suffer from limited healthcare infrastructure that forces them to adjust their healthcare needs during spikes in air pollution (Guidetti et al., 2021), or that low-income and minority populations may be more likely to be exposed to pollution, our results should be considered as a lower bound of the true co-benefits that solar generation can bring to developing countries.

This work can be improved in several ways. For example, we lack comprehensive data to explore the impact of solar power generation on global and other airborne emissions beyond $PM_{2.5}$. Future research could employ satellite data to conduct this analysis. Furthermore, our work estimates the impact of solar generation prior to the northern and southern grid interconnection in Chile; identifying the effect once these two grids are interconnected is another potential avenue of research outside the scope of this paper.[37] Finally, complementary insights on the health benefits of renewable sources can be drawn from other health outcomes as well, such as mortality data. These avenues remain open topics for future research.

References

Abel, D., Holloway, T., Harkey, M., Rrushaj, A., Brinkman, G., Duran, P., Janssen, M., and Denholm, P. (2018). Potential air quality benefits from increased solar photovoltaic electricity generation in the eastern United States. *Atmospheric Environment*, 175:65–74.

Anenberg, S. C., Schwartz, J., Shindell, D., Amann, M., Faluvegi, G., Klimont, Z., Janssens-Maenhout, G., Pozzoli, L., Van Dingenen, R., Vignati, E., et al. (2012). Global air quality and health co-benefits of mitigating near-term climate change through methane and black carbon emission controls. *Environmental Health Perspectives*, 120(6):831–839.

Arceo, E., Hanna, R., and Oliva, P. (2016). Does the effect of pollution on infant mortality differ between developing and developed countries? Evidence from Mexico City. *The Economic Journal*, 126(591):257–280.

[37] The *a priori* effect of the interconnection on the health benefits of solar generation is unclear, due to different factors. First, Chile's major population centers are in the south, which would imply greater impacts from solar generation on health. However, solar generation is more likely to occur in the north, given the region's massive solar irradiation compared to southern Chile. Thus, transmission constraints would likely attenuate that benefit. Furthermore, because the southern grid is cleaner, the relative benefits of solar generation will be lower compared to that in northern Chile. Thus, the overall effect may be larger or smaller than the effect of solar only within SING.

Baker, E., Fowlie, M., Lemoine, D., and Reynolds, S. S. (2013). The economics of solar electricity. *Annu. Rev. Resour. Econ.*, 5(1):387–426.

Banzhaf, S., Ma, L., and Timmins, C. (2019). Environmental justice: The economics of race, place, and pollution. *Journal of Economic Perspectives*, 33(1):185–208.

Barbose, G., Wiser, R., Heeter, J., Mai, T., Bird, L., Bolinger, M., Carpenter, A., Heath, G., Keyser, D., Macknick, J., et al. (2016). A retrospective analysis of benefits and impacts of US renewable portfolio standards. *Energy Policy*, 96:645–660.

Barrows, G., Garg, T., and Jha, A. (2018). The economic benefits versus environmental costs of India's coal-fired power plants. *Available at SSRN*.

Bateson, T. F. and Schwartz, J. (2007). Children's response to air pollutants. *Journal of Toxicology and Environmental Health, Part A*, 71(3):238–243.

Bell, M. L., Dominici, F., and Samet, J. M. (2005). A meta-analysis of time-series studies of Ozone and mortality with comparison to the national morbidity, mortality, and air pollution study. *Epidemiology*, 16(4):436–445.

Bell, M. L., McDermott, A., Zeger, S. L., Samet, J. M., and Dominici, F. (2004). Ozone and short-term mortality in 95 US urban communities, 1987-2000. *JAMA*, 292(19):2372–2378.

Bharadwaj, P., Gibson, M., Zivin, J. G., and Neilson, C. (2017). Gray matters: Fetal pollution exposure and human capital formation. *Journal of the Association of Environmental and Resource Economists*, 4(2):505–542.

Brook, R. D., Rajagopalan, S., Pope III, C. A., Brook, J. R., Bhatnagar, A., Diez-Roux, A. V., Holguin, F., Hong, Y., Luepker, R. V., Mittleman, M. A., et al. (2010). Particulate matter air pollution and cardiovascular disease: an update to the scientific statement from the American Heart Association. *Circulation*, 121(21):2331–2378.

Buonocore, J. J., Luckow, P., Norris, G., Spengler, J. D., Biewald, B., Fisher, J., and Levy, J. I. (2016). Health and climate benefits of different energy-efficiency and renewable energy choices. *Nature Climate Change*, 6(1):100–105.

Burney, J. A. (2020). The downstream air pollution impacts of the transition from coal to natural gas in the United States. *Nature Sustainability*, pages 1–9.

Bushnell, J. and Novan, K. (2021). Setting with the sun: The impacts of renewable energy on conventional generation. *Journal of the Association of Environmental and Resource Economists*, 8(4):759–796.

Callaway, D. S., Fowlie, M., and McCormick, G. (2018). Location, location, location: The variable value of renewable energy and demand-side efficiency resources. *Journal of the Association of Environmental and Resource Economists*, 5(1):39–75.

Carlson, C. L. and Adriano, D. C. (1993). Environmental impacts of coal combustion residues. *Journal of Environmental quality*, 22(2):227–247.

Casey, J. A., Gemmill, A., Karasek, D., Ogburn, E. L., Goin, D. E., and Morello-Frosch, R. (2018a). Increase in fertility following coal and oil power plant retirements in California. *Environmental Health*, 17(1):44.

Casey, J. A., Karasek, D., Ogburn, E. L., Goin, D. E., Dang, K., Braveman, P. A., and Morello-Frosch, R. (2018b). Retirements of coal and oil power plants in California: Association with reduced preterm birth among populations nearby. *American Journal of Epidemiology*, 187(8):1586–1594.

Chauhan, A. J., Inskip, H. M., Linaker, C. H., Smith, S., Schreiber, J., Johnston, S. L., and Holgate, S. T. (2003). Personal exposure to Nitrogen Dioxide (NO_2) and the severity of virus-induced asthma in children. *The Lancet*, 361(9373):1939–1944.

Chay, K. Y. and Greenstone, M. (2003a). Air quality, infant mortality, and the Clean Air Act of 1970. Technical report, National Bureau of Economic Research.

Chay, K. Y. and Greenstone, M. (2003b). The impact of air pollution on infant mortality: Evidence from geographic variation in pollution shocks induced by a recession. *The Quarterly Journal of Economics*, 118(3):1121–1167.

Chen, Y., Ebenstein, A., Greenstone, M., and Li, H. (2013). Evidence on the impact of sustained exposure to air pollution on life expectancy from China's Huai River policy. *Proceedings of the National Academy of Sciences of the United States of America*, 110(32):12936–12941.

Chile Environmental Ministry (2017). Informe Consolidado de Emisiones y Transferencia de Contaminantes 2005-2017. Retrieved from RETC, Ministerio de Medio Ambiente: ttps://retc.mma.gob.cl.

Chile Environmental Ministry (2018). Tercer Informe Bienal de Actualización de Chile sobre Cambio Climático. Retrieved from Ministerio de Medio Ambiente: https://www.mma.gob.cl.

Comisión Nacional de Energía (2018). Anuario Estadístico de Energía. Retrieved from Comisión Nacional de Energía: https://www.cne.cl.

Coneus, K. and Spiess, C. K. (2010). Pollution exposure and infant health: Evidence from Germany. *ZEW-Centre for European Economic Research Discussion Paper*, (10-079).

Cullen, J. (2013). Measuring the environmental benefits of wind-generated electricity. *American Economic Journal: Economic Policy*, 5(4):107–33.

Cullen, J. A. and Mansur, E. T. (2017). Inferring carbon abatement costs in electricity markets: A revealed preference approach using the shale revolution. *American Economic Journal: Economic Policy*, 9(3):106–33.

Currie, J. and Neidell, M. (2005). Air pollution and infant health: What can we learn from California's recent experience? *Quarterly Journal of Economics*, 120(3):1003–1030.

Currie, J., Neidell, M., and Schmieder, J. F. (2009). Air pollution and infant health: Lessons from New Jersey. *Journal of Health Economics*, 28(3):688–703.

Currie, J. and Walker, R. (2011). Traffic congestion and infant health: Evidence from E-ZPass. *American Economic Journal: Applied Economics*, 3(1):65–90.

Currie, J., Zivin, J. G., Mullins, J., and Neidell, M. (2014). What do we know about short-and long-term effects of early-life exposure to pollution? *Annu. Rev. Resour. Econ.*, 6(1):217–247.

Dardati, E., de Elejalde, R., and Giolito, E. P. (2021). On the short-term impact of pollution: The effect of PM 2.5 on emergency room visits.

Edenhofer, O., Hirth, L., Knopf, B., Pahle, M., Schlömer, S., Schmid, E., and Ueckerdt, F. (2013). On the economics of renewable energy sources. *Energy Economics*, 40:S12–S23.

Fell, H. and Kaffine, D. T. (2018). The fall of coal: Joint impacts of fuel prices and renewables on generation and emissions. *American Economic Journal: Economic Policy*, 10(2):90–116.

Fell, H., Kaffine, D. T., and Novan, K. (2021). Emissions, transmission, and the environmental value of renewable energy. *American Economic Journal: Economic Policy*, 13(2):241–72.

Fell, H. and Linn, J. (2013). Renewable Electricity Policies, Heterogeneity, and Cost Effectiveness. *Journal of Environmental Economics and Management*, 66(3):688–707.

Franklin, B. A., Brook, R., and Pope III, C. A. (2015). Air pollution and cardiovascular disease. *Current Problems in Cardiology*, 40(5):207–238.

Galetovic, A. and Muñoz, C. M. (2011). Regulated electricity retailing in Chile. *Energy Policy*, 39(10):6453–6465.

Gauderman, W. J., Avol, E., Lurmann, F., Kuenzli, N., Gilliland, F., Peters, J., and McConnell, R. (2005). Childhood asthma and exposure to traffic and Nitrogen Dioxide. *Epidemiology*, 16(6):737–743.

Guidetti, B., Pereda, P., and Severnini, E. (2021). " placebo tests" for the impacts of air pollution on health: The challenge of limited health care infrastructure. In *AEA Papers and Proceedings*, volume 111, pages 371–75.

Gupta, A. and Spears, D. (2017). Health externalities of India's expansion of coal plants: Evidence from a national panel of 40,000 households. *Journal of Environmental Economics and Management*, 86:262–276.

Haas, J., Palma-Behnke, R., Valencia, F., Araya, P., Díaz-Ferrán, G., Telsnig, T., Eltrop, L., Díaz, M., Püschel, S., Grandel, M., et al. (2018). Sunset or sunrise? understanding the barriers and options for the massive deployment of solar technologies in Chile. *Energy Policy*, 112:399–414.

Hoek, G., Krishnan, R. M., Beelen, R., Peters, A., Ostro, B., Brunekreef, B., and Kaufman, J. D. (2013). Long-term air pollution exposure and cardio-respiratory mortality: a review. *Environmental Health*, 12(1):43.

Holladay, J. S. and LaRiviere, J. (2017). The impact of cheap natural gas on marginal emissions from electricity generation and implications for energy policy. *Journal of Environmental Economics and Management*, 85:205–227.

Hollingsworth, A. and Rudik, I. (2019). External impacts of local energy policy: The case of renewable portfolio standards. *Journal of the Association of Environmental and Resource Economists*, 6(1):187–213.

Jacques-Coper, M., Falvey, M., and Muñoz, R. C. (2015). Inter-daily variability of a strong thermally-driven wind system over the Atacama Desert of South America: synoptic forcing and short-term predictability using the GFS global model. *Theoretical and Applied Climatology*, 121(1-2):211–223.

Johnsen, R., LaRiviere, J., and Wolff, H. (2019). Fracking, coal, and air quality. *Journal of the Association of Environmental and Resource Economists*, 6(5):1001–1037.

Kaffine, D. T., McBee, B. J., and Lieskovsky, J. (2013). Emissions savings from wind power generation in Texas. *The Energy Journal*, 34(1).

Knittel, C. R., Metaxoglou, K., and Trindade, A. (2015). Natural gas prices and coal displacement: Evidence from electricity markets. Technical report, National Bureau of Economic Research.

Knittel, C. R., Miller, D. L., and Sanders, N. J. (2016). Caution, drivers! Children present: Traffic, pollution, and infant health. *Review of Economics and Statistics*, 98(2):350–366.

Kopas, J., York, E., Jin, X., Harish, S., Kennedy, R., Shen, S. V., and Urpelainen, J. (2020). Environmental justice in India: Incidence of air pollution from coal-fired power plants. *Ecological Economics*, 176:106711.

Lavaine, E. and Neidell, M. (2017). Energy production and health externalities: Evidence from oil refinery strikes in France. *Journal of the Association of Environmental and Resource Economists*, 4(2):447–477.

Linn, J., Mastrangelo, E., and Burtraw, D. (2014). Regulating greenhouse gases from coal power plants under the Clean Air Act. *Journal of the Association of Environmental and Resource Economists*, 1(1/2):97–134.

Linn, J. and Muehlenbachs, L. (2018). The heterogeneous impacts of low natural gas prices on consumers and the environment. *Journal of Environmental Economics and Management*, 89:1–28.

Lu, X., Salovaara, J., and McElroy, M. B. (2012). Implications of the recent reductions in natural gas prices for emissions of CO_2 from the US power sector. *Environmental Science & Technology*, 46(5):3014–3021.

Millstein, D., Wiser, R., Bolinger, M., and Barbose, G. (2017). The climate and air-quality benefits of wind and solar power in the United States. *Nature Energy*, 2(9):17134.

Ministry of Energy (2013). Ley 20.698: Propicia la ampliación de la matriz energética mediante fuentes renovables no convencionales. Retrieved from Congreso Nacional de Chile.

Muller, N. Z. and Mendelsohn, R. (2009). Efficient pollution regulation: getting the prices right. *American Economic Review*, 99(5):1714–39.

Muñoz, R. C., Falvey, M. J., Arancibia, M., Astudillo, V. I., Elgueta, J., Ibarra, M., Santana, C., and Vásquez, C. (2018). Wind energy exploration over the Atacama Desert: A numerical model–guided observational program. *Bulletin of the American Meteorological Society*, 99(10):2079–2092.

Neidell, M. (2009). Information, avoidance behavior, and health the effect of Ozone on asthma hospitalizations. *Journal of Human Resources*, 44(2):450–478.

Novan, K. (2015). Valuing the wind: Renewable energy policies and air pollution avoided. *American Economic Journal: Economic Policy*, 7(3):291–326.

Orehek, J., Massari, J. P., Gayrard, P., Grimaud, C., and Charpin, J. (1976). Effect of short-term, low-level Nitrogen Dioxide exposure on bronchial sensitivity of asthmatic patients. *Journal of Clinical Investigation*, 57(2):301–307.

Pershagen, G., Rylander, E., Norberg, S., Eriksson, M., and Nordvall, S. L. (1995). Air pollution involving Nitrogen Dioxide exposure and Wheezing Bronchitis in children. *International Journal of Epidemiology*, 24(6):1147–1153.

Programa Chile Sustentable (2017). Termoelétricas a Carbón en Chile. http://www.chilesustentable.net. Retrieved in March, 2020.

Rau, T., Urzúa, S., and Reyes, L. (2015). Early exposure to hazardous waste and academic achievement: evidence from a case of environmental negligence. *Journal of the Association of Environmental and Resource Economists*, 2(4):527–563.

Rivera, N. M. (2020). Is mining an environmental disamenity? evidence from resource extraction site openings. *Environmental and Resource Economics*, 75(3):485–528.

Rondanelli, R., Molina, A., and Falvey, M. (2015). The Atacama surface solar maximum. *Bulletin of the American Meteorological Society*, 96(3):405–418.

Ruiz-Rudolph, P., Arias, N., Pardo, S., Meyer, M., Mesías, S., Galleguillos, C., Schiattino, I., and Gutiérrez, L. (2016). Impact of large industrial emission sources on mortality and morbidity in Chile: A small-areas study. *Environment International*, 92:130–138.

Schlenker, W. and Walker, W. R. (2016). Airports, air pollution, and contemporaneous health. *The Review of Economic Studies*, 83(2):768–809.

Schwartz, J. (1996). Air pollution and hospital admissions for respiratory disease. *Epidemiology*, pages 20–28.

Schwartz, J. and Morris, R. (1995). Air pollution and hospital admissions for cardiovascular disease in Detroit, Michigan. *American Journal of Epidemiology*, 142(1):23–35.

Sergi, B., Adams, P. J., Muller, N., Robinson, A. L., Davis, S., Marshall, J. D., and Azevedo, I. M. L. (2020). Optimizing emissions reductions from the US power sector for climate and health benefits. *Environmental Science & Technology*.

Siler-Evans, K., Azevedo, I. L., Morgan, M. G., and Apt, J. (2013). Regional variations in the health, environmental, and climate benefits of wind and solar generation. *Proceedings of the National Academy of Sciences*, 110(29):11768–11773.

Spiller, E., Sopher, P., Martin, N., Mirzatuny, M., and Zhang, X. (2017). The environmental impacts of green technologies in TX. *Energy Economics*, 68:199–214.

Stocker, T. F., Qin, D., Plattner, G.-K., Tignor, M., Allen, S. K., Boschung, J., Nauels, A., Xia, Y., Bex, V., Midgley, P. M., et al. (2013). Climate change 2013: The physical science basis. *Contribution of Working Group I to the Fifth Assessment Report of the Intergovernmental Panel on Climate Change*, 1535.

Thakrar, S. K., Balasubramanian, S., Adams, P. J., Azevedo, I. M., Muller, N. Z., Pandis, S. N., Polasky, S., Pope III, C. A., Robinson, A. L., Apte, J. S., et al. (2020). Reducing mortality from air pollution in the united states by targeting specific emission sources. *Environmental Science & Technology Letters*, 7(9):639–645.

U.S. Energy Information Administration (2019). International Energy Outlook 2019. Retrieved in November, 2019.

U.S. Environmental Protection Agency (2006). Air quality criteria document for Ozone. https://cfpub.epa.gov/ncea/risk/recordisplay.cfm?deid=149923. Retrieved in December, 2020.

U.S. Environmental Protection Agency (2014). EPA's Report on the Environment (ROE): Sulfur Dioxide Emissions. https://cfpub.epa.gov/roe/indicator.cfm?i=22. Last Updated: 2014.

U.S. Environmental Protection Agency (2019). Local Renewable Energy Benefits and Resources. https://www.epa.gov/statelocalenergy/local-renewable-energy-benefits-and-resources. Retrieved in November, 2019.

Wiser, R., Mai, T., Millstein, D., Barbose, G., Bird, L., Heeter, J., Keyser, D., Krishnan, V., and Macknick, J. (2017). Assessing the costs and benefits of US renewable portfolio standards. *Environmental Research Letters*, 12(9):094023.

Wooldridge, J. M. (2010). *Econometric analysis of cross section and panel data*. MIT press.

World Health Organization (2006). *Air Quality Guidelines*. Global Update 2005. World Health Organization.

Appendix

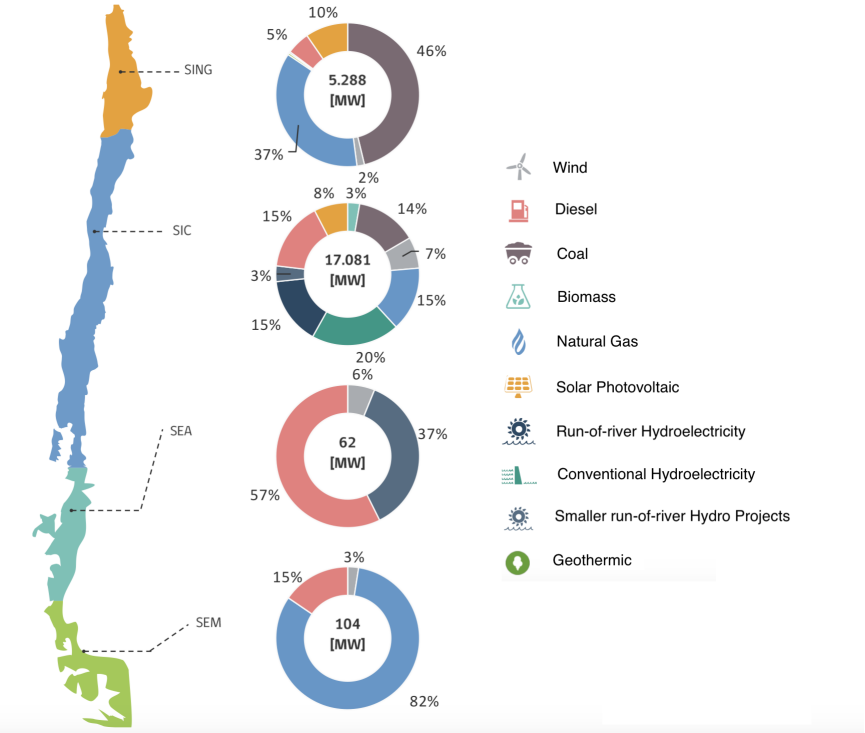

Figure A1: Bulk Power Systems in Chile

Notes: This figure depicts the four bulk power system that existed in Chile until 2018. It also displays the fuel source composition of each system: the Northern Interconnected System (SING), the Central Interconnected System (SIC), the Aysen Electric System (SEA), and the Magallanes Electric System (SEM). SING and SIC interconnected in 2018, and the whole system was renamed as the National Electric System (SEC). This figure was adapted from the *National Energy Commission Monthly Report*, dated December 2017. https://www.cne.cl/wp-content/uploads/2015/06/RMensual_v201712.pdf

Table A1: Monthly Fuel Use and Prices

Variable	Mean	Std. Dev.	Min.	Max.	Obs.
Panel A. Fuel Use					
Coal	34,931.76	3,210.30	25,949.25	42,148.77	2,192
Diesel	1,020.77	684.61	26.08	2,602.4	2,192
Fuel oil	369.33	301.059	1	1,219	1,187
Fuel oil #6	955.93	910.55	9	3,321.5	2,192
Natural gas	15,333.87	7,389.24	3,371.79	44,707.66	2,192
Panel B. Fuel Prices					
Coal	105.41	16.21	68.19	138.73	2,192
Diesel	620.94	200.63	288.5	908.7	2,192
Fuel oil	95.79	22.91	46.67	125.33	1,187
Fuel oil #6	446.96	175.40	157	728.41	2,192
Natural gas	3.15	0.79	1.7	5.94	2,192

Notes: This table displays main descriptive statistics of monthly fossil fuel uses and prices from 2012 to 2017. Descriptive statistics use main fuel source only. Coal, diesel and fuel oil are in tons, while natural gas is in thousands m^3. Prices are in US$/ton for coal, US$/m^3 for diesel and fuel oil #6, in US$/mm btu for natural gas, and in US$/bbl for fuel oil. Data come from the National Energy Commission.

Table A2: Summary Statistics on the Daily Rate of Hospital Admissions by Age Group

Disease	Mean	Std. Dev.	Min.	Max.	Obs.
Panel A. Infants					
Cardiovascular	0.004	0.436	0	85.324	41,648
All respiratory	0.126	1.058	0	78.309	41,648
Upper respiratory	0.007	0.212	0	29.326	41,648
Lower respiratory	0.116	1.027	0	78.309	41,648
Panel B. Toddlers					
Cardiovascular	0.004	0.138	0	19.372	41,648
All respiratory	0.235	1.956	0	107.759	41,648
Upper respiratory	0.079	0.812	0	57.937	41,648
Lower respiratory	0.150	1.759	0	107.759	41,648
Panel C. Kids					
Cardiovascular	0.012	0.387	0	58.893	41,648
All respiratory	0.128	2.555	0	319.489	41,648
Upper respiratory	0.065	0.930	0	85.324	41,648
Lower respiratory	0.061	2.375	0	319.489	41,648
Panel D. Adults					
Cardiovascular	0.535	3.337	0	409.836	41,648
All respiratory	0.364	2.290	0	168.350	41,648
Upper respiratory	0.119	1.383	0	168.350	41,648
Lower respiratory	0.190	1.677	0	107.759	41,648
Panel E. Seniors					
Cardiovascular	0.489	3.418	0	322.581	41,648
All respiratory	0.350	3.728	0	409.836	41,648
Upper respiratory	0.006	0.339	0	56.465	41,648
Lower respiratory	0.27	2.457	0	107.759	41,648

Notes: This table displays main descriptive statistics of the daily rate of hospital admissions by age group from 2012 to 2017. Hospital admission rates are per 100,000 people. Observations are across all cities in the sample using patient's city of origin. Data come from the Ministry of Health, through the Department of Health Statistics and Information (DEIS) from 2012 to 2017.

Table A3: Descriptive Statistics - Other Covariates

Variable	Mean	Std. Dev.	Min.	Max.
Panel A. All cities (n= 19)				
Demographics:				
Population	61,802.89	104,603.38	244	395,453
Density	19.43	47.45	0.08	229.51
Poverty Rate	14.11	9.06	2	37
Fertility Rate	11.18	6.32	0	21.6
Weather:				
Min. Temp. (C)	7.10	6.34	-25	23
Max. Temp. (C)	10.72	8.65	-11.8	33.4
Humidity (%)	49.11	13.71	9.68	96.26
Panel B. Cities with fossil fuel generation (n= 5)				
Demographics:				
Population	167,575	140,344.43	11,090	395,453
Density	30.91	32.35	2.92	89.28
Poverty Rate	8.30	3.66	3.12	15.71
Fertility Rate	16.31	2.13	12.19	21.6
Weather:				
Min. Temp. (C)	9.03	6.67	-18.4	23
Max. Temp. (C)	13.46	8.72	-11.8	33.4
Humidity (%)	52.31	14.07	9.69	96.26
Panel C. Cities without fossil fuel generation (n = 13)				
Demographics:				
Population	25,041.19	51,812.2	244	184,543
Density	16.42	53.11	0.08	229.51
Poverty Rate	16.29	9.82	2	37
Fertility Rate	9.40	6.49	0	20.99
Weather:				
Min. Temp. (C)	6.40	6.09	-25	22
Max. Temp. (C)	9.98	8.52	-11.8	33
Humidity (%)	47.88	13.68	9.68	95.85

Notes: This table displays main descriptive statistics of covariates by groups of cities. Observations are at the city level. There is one city in our sample, Pica, that switches from panel C to panel B due to the opening of a new fossil fuel generator during our study period. We discard this city from panels B and C. Data comes from the National System of Municipalities Information (SINIM) from 2012 to 2017.

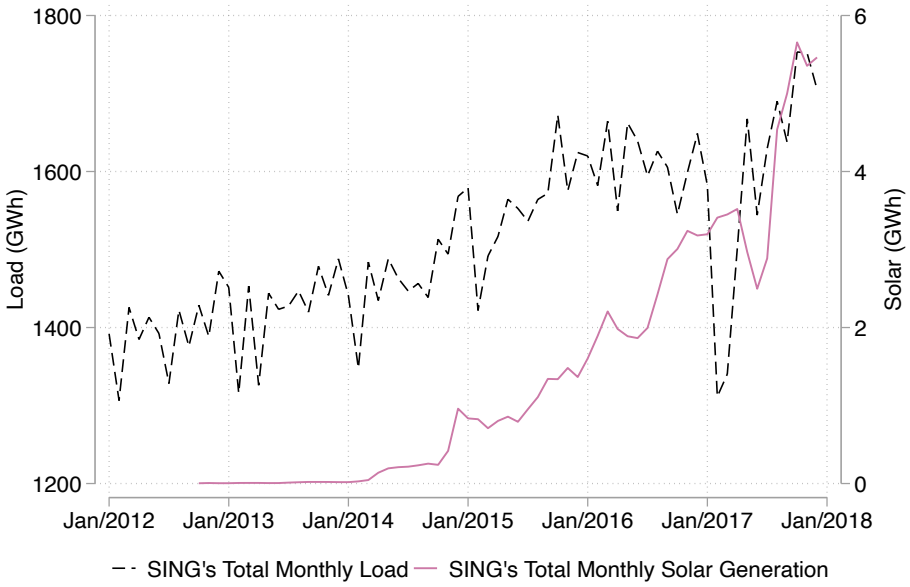

Figure A2: SING's Monthly Load and Solar Generation

Notes: This figure depicts the total monthly load and total monthly solar power generation at SING. Information is in gigawatts per hour (GWh). Monthly load is on the main y-axis. Monthly solar generation is on the secondary y-axis. Data comes from the National Electricity Coordinator from 2012 to 2017.

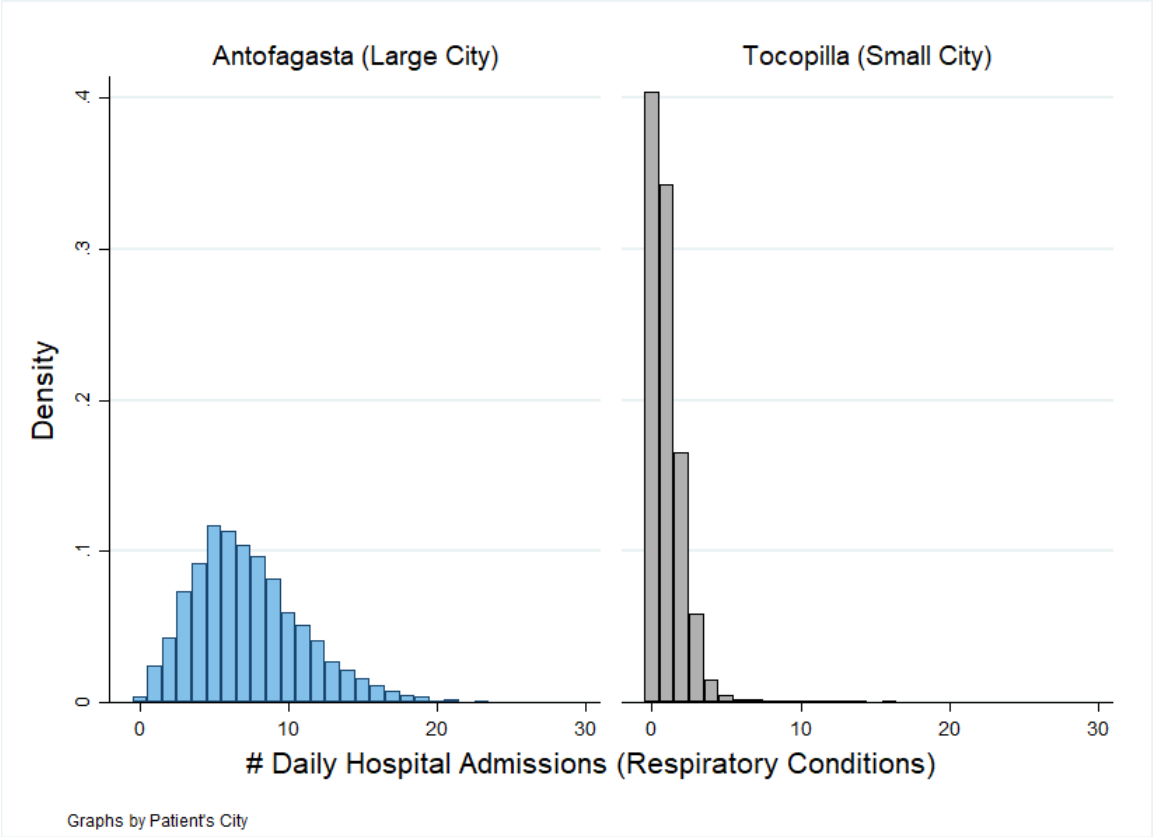

Figure A3: Overdispersion in the Health Outcome Variables

Notes: The left-hand panel exhibits the number of daily hospital admissions due to respiratory conditions for one of the largest cities in the sample, Antofagasta, while the right-hand panel shows the same variable for the case of a smaller city, Tocopilla. The overdispersion of this variable is evident in the case of the large city (left-hand side). The heterogeneity in the size of the pile-up at zero is also clear when comparing the two cities.

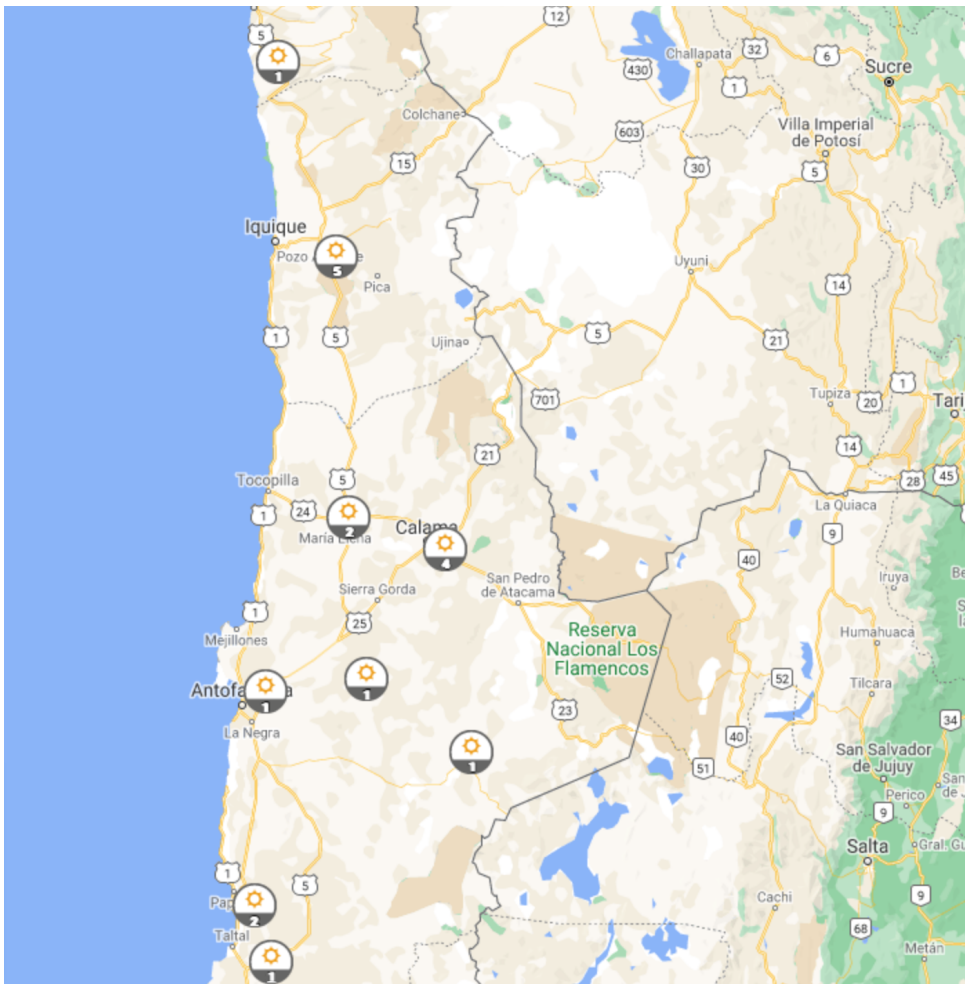

Figure A4: Location of Solar Generators at SING

Notes: This figure depicts the location of the solar generators at SING (northern Chile) included in our analysis. The figure was obtained from the National Energy Comission (CNE) from https://energiamaps.cne.cl

Table A4: The Effect of 1 GWh of Solar Power Generation on Daily Aggregated Renewable Generation

	Wind		Hydro		Geothermal	
	(1)	(2)	(1)	(2)	(1)	(2)
Panel A. Generation (GWh)						
Solar_d	0.015	0.099***	-0.008***	-0.007***	-0.071***	-0.026
	(0.020)	(0.019)	(0.001)	(0.002)	(0.019)	(0.016)
Panel B. Capacity Factor						
Solar_d	-0.004	0.013**	-0.021***	-0.018***	-0.050***	-0.040***
	(0.005)	(0.004)	(0.004)	(0.005)	(0.013)	(0.011)
Obs.	1,489	1,489	1,915	1,915	306	306
Controls	✓	✓	✓	✓	✓	✓
τ_1 fixed effects	✓		✓		✓	
τ_2 fixed effects		✓		✓		✓

Notes: This table displays estimation results from regressions of daily aggregated renewable generation (panel A) and renewables' daily capacity factors (panel B) on daily solar power generation. Estimation results are marginal effects of daily solar generation (in GWh) derived from an OLS on daily aggregated generation, and from a fractional logit response model on daily capacity factors. All estimations include plants with both single- and dual-fuel engines. All regressions include daily temperature, humidity and load as controls (fuel price ratios are not included in this regression as these are renewable generators only). Vector τ_1 includes year, month, and weekend fixed effects. Vector τ_2 includes year, seasons, year $\times$ seasons, and weekend fixed effects. Bootstrapped standard errors appear in parentheses. Significance levels: $^{*}p < 0.10$, $^{**}p < 0.05$, $^{***}p < 0.001$.

Table A5: The Effect of Solar on Daily Aggregated Fossil Fuel Generation Using Single-Fuel Engines Only

	Coal		Diesel		Fuel oil		Fuel oil #6	
	(1)	(2)	(1)	(2)	(1)	(2)	(1)	(2)
Panel A. Generation (GWh)								
Solar_d	-0.813***	-0.813***	-0.017	-0.017	-0.011	-0.011	0.001	0.001
	(0.137)	(0.137)	(0.011)	(0.011)	(0.023)	(0.023)	(0.001)	(0.001)
Panel B. Capacity Factor								
Solar_d	-0.022***	-0.022***	-0.009**	-0.009**	0.047	0.047	0.029	0.029
	(0.004)	(0.004)	(0.004)	(0.004)	(0.047)	(0.047)	(0.018)	(0.018)
Obs.	1,915	1,915	1,915	1,915	910	910	1,825	1,825
Controls	✓	✓	✓	✓	✓	✓	✓	✓
τ_1 fixed effects	✓		✓		✓		✓	
τ_2 fixed effects		✓		✓		✓		✓

Notes: This table displays estimation results from regressions of daily aggregated fossil fuel generation (panel A) and fossil fuels' daily capacity factors (panel B) on daily solar power generation. Estimation results are marginal effects of daily solar generation (in GWh) derived from an OLS regression on daily aggregated generation, and from a fractional logit response model on daily capacity factors. All estimations include plants with both single- and dual-fuel engines. All regressions include daily temperature, humidity, load and price ratios as controls. Vector τ_1 includes year, month, and weekend fixed effects. Vector τ_2 includes year, seasons, year $\times$ seasons, and weekend fixed effects. Bootstrapped standard errors appear in parentheses. Significance levels: $^{*}p < 0.10$, $^{**}p < 0.05$, $^{***}p < 0.001$.

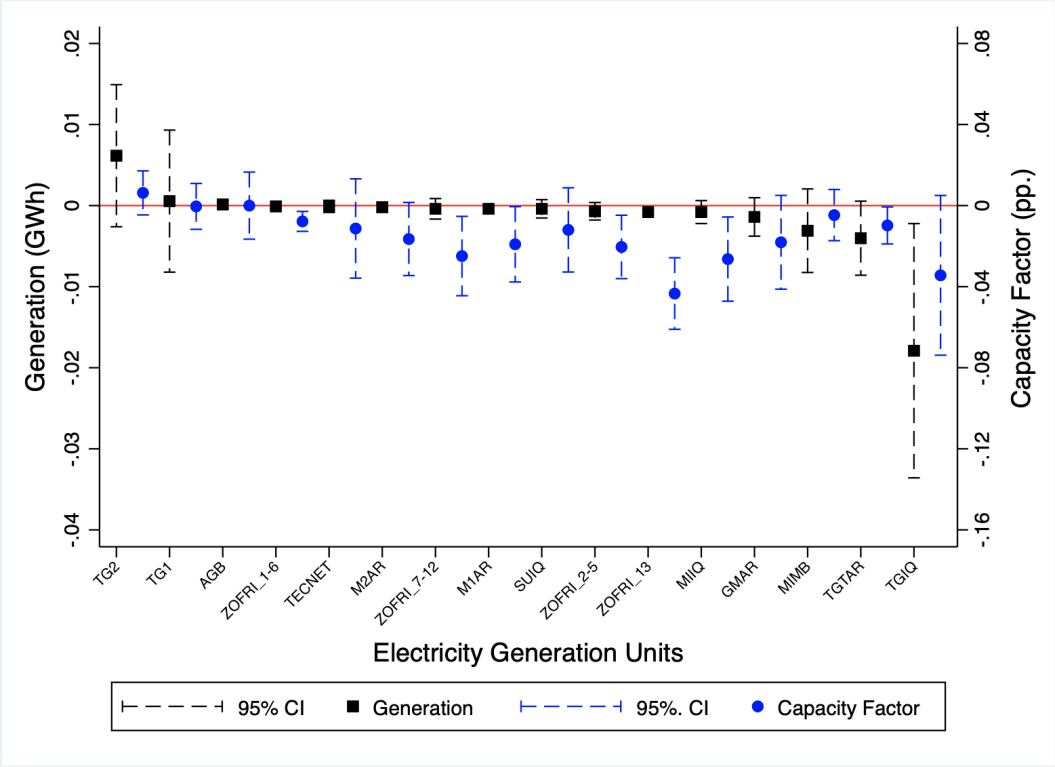

Figure A5: Diesel-Fired (Single-Fuel) EGUs and Displacement

Notes: The figure shows estimation results from regressions of daily diesel-fired generation (squares) and capacity factors (circles) on daily solar power generation at the electricity generation unit (EGU) level. Point estimates are marginal effects of daily solar generation (in GWh) derived from an OLS on daily aggregated generation (left y-axis), and from a fractional logit response model on daily capacity factors (right y-axis). The estimation equations are identical to the ones in columns (2) of Table 3. Dashed lines represent 95% confidence intervals obtained with bootstrapped standard errors. Reference line in red is at the zero mark. All estimations use combined-cycle EGUs that report diesel as their primary fuel source. We exclude units with dual engines that run with natural gas or that report using fuel oil as well.

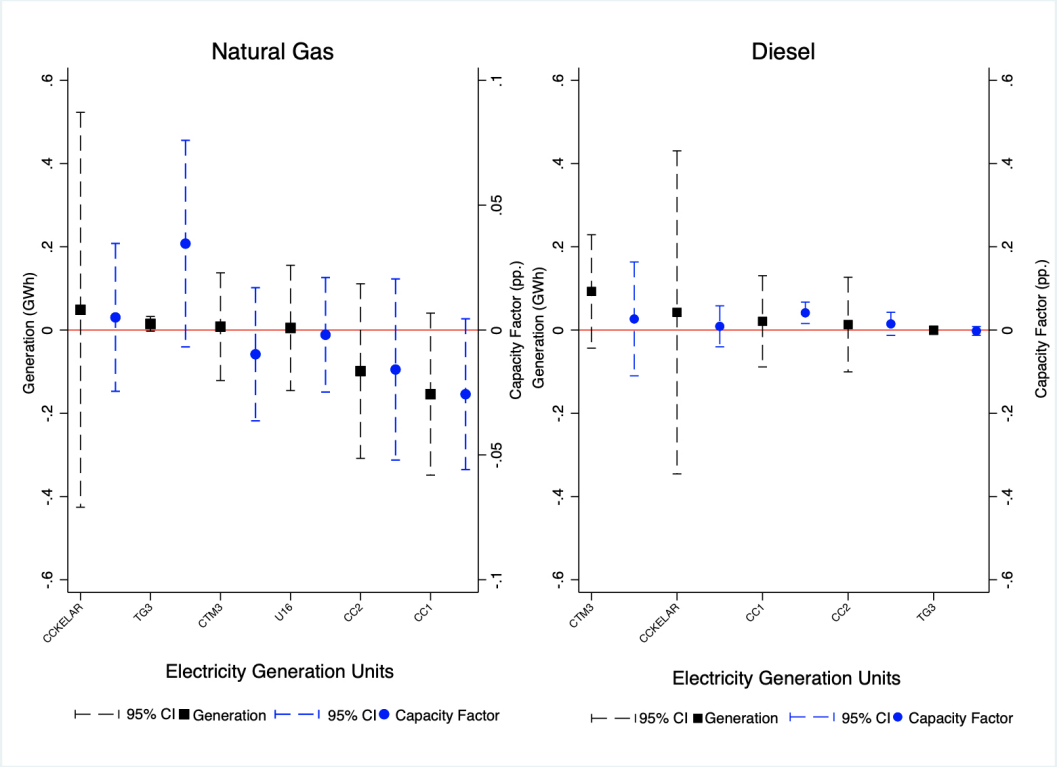

Figure A6: Natural Gas-Fired (Combined-Cycle) EGUs and Displacement

Notes: The figure shows estimation results from regressions of daily gas-fired generation (squares) and capacity factors (circles) on daily solar power generation at the electricity generation unit (EGU) level. Natural gas-fired plants in our sample are all combined-cycle plants. The left-hand side graph shows estimation results for gas plants. The right-hand side graph shows estimation results for diesel plants. Point estimates are marginal effects of daily solar generation (in GWh) derived from an OLS regression on daily aggregated generation (left y-axis), and from a fractional logit response model on daily capacity factors (right y-axis). The estimation equations are identical to the ones in columns (2) of Table 3. Dashed lines represent 95% confidence intervals obtained with bootstrapped standard errors. Reference line in red is at the zero mark. All estimations use combined-cycle EGUs that report natural gas as their primary fuel source.

Table A6: The Effect of Daily Solar Generation on the Daily Rate of Hospital Admissions by Age Group – All Cities

	All Cities									
	Infants		Toddlers		Kids		Adults		Seniors	
	(1)	(2)	(1)	(2)	(1)	(2)	(1)	(2)	(1)	(2)
Panel A. Cardiovascular										
Solar_d	0.00002	-0.0001	-0.0002	-0.0002	-0.0030***	-0.0027**	-0.0056	-0.0077	-0.0155	-0.0148
	(0.0002)	(0.0024)	(0.0014)	(0.0011)	(0.0007)	(0.0010)	(0.0057)	(0.0084)	(0.0096)	(0.0097)
Panel B. All Respiratory										
Solar_d	-0.0206***	-0.0201***	-0.0232***	-0.0228	-0.0042	-0.0039	-0.0073*	-0.0127	-0.0126***	-0.0112***
	(0.0051)	(0.0050)	(0.0065)	(0.0246)	(0.0074)	(0.0071)	(0.0044)	(0.0113)	(0.0017)	(0.0015)
Panel C. Upper Respiratory										
Solar_d	0.0005	0.0004	-0.0032	-0.0035	-0.0104**	-0.0110**	-0.0112**	-0.0111	-0.0014***	-0.0013***
	(0.0011)	(0.0015)	(0.0036)	(0.0163)	(0.0046)	(0.0040)	(0.0036)	(0.0168)	(0.0004)	(0.0003)
Panel D. Lower Respiratory										
Solar_d	-0.0221***	-0.0214***	-0.0171	-0.0145***	0.0052*	0.0046	0.0021	0.0006	-0.0102***	-0.0091***
	(0.0053)	(0.0055)	(0.0462)	(0.0035)	(0.0028)	(0.0033)	(0.0027)	(0.0042)	(0.0021)	(0.0019)
Obs.	36,385	36,385	36,385	36,385	36,385	36,385	36,385	36,385	36,385	36,385
Number of Cities	19	19	19	19	19	19	19	19	19	19
Controls	✓	✓	✓	✓	✓	✓	✓	✓	✓	✓
City fixed effects	✓		✓		✓		✓		✓	
City×Year fixed effects		✓		✓		✓		✓		✓

Notes: This table displays estimation results from regressions of daily hospital admissions on daily solar power generation across all cities by age group. Solar generation is in GWh. Estimation results are marginal effects from ZINB regressions offsetting by population. Controls include weather, mining production, and demographic covariates. All regressions include controls, year, seasons, year × seasons, and weekend fixed effects in both the main and the inflate equations. Clustered standard errors by city appear in parentheses. Significance levels: $^{*}p < 0.10$, $^{**}p < 0.05$, $^{***}p < 0.001$.

Table A7: The Effect of Daily Solar Generation on the Daily Rate of Hospital Admissions by Age Group – Cities Downwind $10km$

	Cities Downwind of Displaced Fossil Fuel Plants Within 10km									
	Infants		Toddlers		Kids		Adults		Seniors	
	(1)	(2)	(1)	(2)	(1)	(2)	(1)	(2)	(1)	(2)
Panel A. Cardiovascular										
Solar_d	0.0004**	0.0004	-0.0005	-0.0010	-0.0026	-0.0029	-0.0330	-0.0197	-0.0240	-0.0281
	(0.0002)	(0.0004)	(0.0060)	(0.0040)	(0.0059)	(0.0041)	(0.0742)	(0.0380)	(0.0578)	(0.0243)
Panel B. All Respiratory										
Solar_d	-0.0529*	-0.0531***	-0.0354	-0.0386	-0.0028	-0.0010	-0.0142	-0.0154	-0.0157**	-0.0149***
	(0.0306)	(0.0053)	(0.0318)	(0.0287)	(0.0275)	(0.0321)	(0.0597)	(0.0221)	(0.0077)	(0.0042)
Panel C. Upper Respiratory										
Solar_d	0.0006	0.0008	-0.0137**	-0.0118	-0.0131	-0.0134	-0.0032	-0.0030	-0.0020	-0.0022
	(0.0772)	(0.0057)	(0.0061)	(0.0152)	(0.0084)	(0.0148)	(0.0296)	(0.0038)	(0.388)	(17.61)
Panel D. Lower Respiratory										
Solar_d	-0.0540***	-0.0599	-0.0311**	-0.0327*	-0.0047***	-0.0038**	-0.0285	-0.0197	-0.0188***	-0.0175***
	(0.0160)	(0.0515)	(0.0124)	(0.0190)	(0.0003)	(0.0014)	(0.966)	(0.0197)	(0.0008)	(0.0027)
Obs.	3,830	3,830	3,830	3,830	3,830	3,830	3,830	3,830	3,830	3,830
Number of Cities	2	2	2	2	2	2	2	2	2	2
Controls	✓	✓	✓	✓	✓	✓	✓	✓	✓	✓
City fixed effects	✓		✓		✓		✓		✓	
City×Year fixed effects		✓		✓		✓		✓		✓

Notes: This table displays estimation results from regressions of daily hospital admissions on daily solar power generation across cities downwind $10km$ by age group. Solar generation is in GWh. Estimation results are marginal effects from ZINB regressions offsetting by population. Controls include weather, mining production, and demographic covariates. All regressions include controls, year, seasons, year × seasons, and weekend fixed effects in both the main and the inflate equations. Clustered standard errors by city appear in parentheses. Significance levels: $^{*}p < 0.10$, $^{**}p < 0.05$, $^{***}p < 0.001$.

Table A8: The Effect of Daily Solar Generation on the Daily Rate of Hospital Admissions by Age Group – Cities Downwind $50km$

	Cities Downwind of Displaced Fossil Fuel Plants Within 10km									
	Infants		Toddlers		Kids		Adults		Seniors	
	(1)	(2)	(1)	(2)	(1)	(2)	(1)	(2)	(1)	(2)
Panel A. Cardiovascular										
Solar_d	-0.0002	0.0002	-0.0006	-0.0005	-0.0015	-0.0017	-0.0204	-0.0258	-0.0134	-0.0132
	(0.0015)	(0.0516)	(0.0033)	(0.0114)	(0.0024)	(0.0033)	(0.0285)	(0.0233)	(0.0196)	(0.0541)
Panel B. All Respiratory										
Solar_d	-0.0361***	-0.0351***	-0.0219	-0.0190	-0.0049	-0.0032	-0.0037	-0.0023	-0.0140**	-0.0126**
	(0.0058)	(0.0061)	(0.0199)	(0.0222)	(0.0310)	(0.0516)	(0.112)	(0.158)	(0.0056)	(0.0064)
Panel C. Upper Respiratory										
Solar_d	-0.0001	-0.0027	-0.0073	-0.0086	-0.0121**	-0.0131***	0.0024	0.0009	-0.0056	-23414.0
	(0.0045)	(2.108)	(0.0050)	(0.0064)	(0.0051)	(0.0030)	(0.0055)	(0.0057)	(0.0035)	(8323629.2)
Panel D. Lower Respiratory										
Solar_d	-0.0363***	-0.0327	-0.0197	-0.0182	-0.0025*	-0.0023**	-0.0136	-0.0090	-0.0123	-0.0139
	(0.0064)	(0.0246)	(0.0146)	(0.0142)	(0.0013)	(0.0008)	(0.0353)	(0.0116)	(0.0076)	(0.0135)
Obs.	5,745	5,745	5,745	5,745	5,745	5,745	5,745	5,745	5,745	5,745
Number of Cities	3	3	3	3	3	3	3	3	3	3
Controls	✓	✓	✓	✓	✓	✓	✓	✓	✓	✓
City fixed effects	✓		✓		✓		✓		✓	
City×Year fixed effects		✓		✓		✓		✓		✓

Notes: This table displays estimation results from regressions of daily hospital admissions on daily solar power generation across cities downwind $50km$ by age group. Solar generation is in GWh. Estimation results are marginal effects from ZINB regressions offsetting by population. Controls include weather, mining production, and demographic covariates. All regressions include controls, year, seasons, year × seasons, and weekend fixed effects in both the main and the inflate equations. Clustered standard errors by city appear in parentheses. Significance levels: $^{*}p < 0.10$, $^{**}p < 0.05$, $^{***}p < 0.001$.

Table A9: The Effect of Daily Solar Generation on the Daily Rate of Hospital Admissions by Age Group – Cities Downwind $100km$

	Cities Downwind of Displaced Fossil Fuel Plants Within 100km									
	Infants		Toddlers		Kids		Adults		Seniors	
	(1)	(2)	(1)	(2)	(1)	(2)	(1)	(2)	(1)	(2)
Panel A. Cardiovascular										
$Solar_d$	-0.0002	0.0001	-0.0004	-0.0005	-0.0011	-0.0013	-0.0205	-0.0266	-0.0070	-0.0078
	(0.0003)	(0.0004)	(0.0057)	(0.0021)	(0.0022)	(0.0020)	(0.0162)	(0.0720)	(0.0095)	(0.0161)
Panel B. All Respiratory										
$Solar_d$	-0.0312**	-0.0265***	-0.0181**	-0.0194**	-0.0104*	-0.0030	-0.0067	-0.0032	-0.0127**	-0.0128**
	(0.0134)	(0.0034)	(0.0078)	(0.0081)	(0.0053)	(0.0102)	(0.0114)	(0.0156)	(0.0056)	(0.0053)
Panel C. Upper Respiratory										
$Solar_d$	0.0013	0.0017	-0.0052	-0.0025	-0.0128***	-0.0096*	-0.0014	-0.0007	-0.0010	-0.0010
	(0.0012)	(0.0019)	(0.0038)	(0.0042)	(0.0038)	(0.0052)	(0.0029)	(0.0031)	(0.0015)	(0.0014)
Panel D. Lower Respiratory										
$Solar_d$	-0.0282***	-0.0255***	-0.0174*	-0.0154	-0.0009	-0.0008	-0.0125	-0.0119	-0.0134**	-0.0104**
	(0.0059)	(0.0070)	(0.0100)	(0.0196)	(0.0014)	(0.0054)	(0.0080)	(0.0100)	(0.0053)	(0.0046)
Obs.	7,660	7,660	7,660	7,660	7,660	7,660	7,660	7,660	7,660	7,660
Number of Cities	4	4	4	4	4	4	4	4	4	4
Controls	✓	✓	✓	✓	✓	✓	✓	✓	✓	✓
City fixed effects	✓		✓		✓		✓		✓	
City×Year fixed effects		✓		✓		✓		✓		✓

Notes: This table displays estimation results from regressions of daily hospital admissions on daily solar power generation across cities downwind $100km$ by age group. Solar generation is in GWh. Estimation results are marginal effects from ZINB regressions offsetting by population. Controls include weather, mining production, and demographic covariates. All regressions include controls, year, seasons, year × seasons, and weekend fixed effects in both the main and the inflate equations. Clustered standard errors by city appear in parentheses. Significance levels: $^{*}p < 0.10$, $^{**}p < 0.05$, $^{***}p < 0.001$.

Table A10: The Long-Term Effect of Average Solar Generation on the Daily Rate of Hospital Admissions

	All Cities			Cities Downwind of Displaced Fossil Fuel Plants								
				$< 10km$			$< 50km$			$< 100km$		
	t=week	t=month	t=year	t=week	t=month	t=year	t=week	t=month	t=year	t=week	t=month	t=year
Panel A. Cardiovascular												
Solar_t	-0.026***	-0.029***	-0.038***	-0.055	-0.066	-0.098	-0.024	-0.029	-0.042**	-0.025*	-0.029**	-0.044**
	(0.005)	(0.007)	(0.009)	(0.052)	(0.052)	(0.071)	(0.019)	(0.018)	(0.019)	(0.015)	(0.014)	(0.017)
Panel B. All respiratory												
Solar_t	-0.034***	-0.026***	-0.020**	-0.072***	-0.023**	0.015	-0.035***	-0.010	0.017	-0.034***	-0.014	0.0004
	(0.007)	(0.006)	(0.008)	(0.008)	(0.010)	(0.043)	(0.010)	(0.010)	(0.023)	(0.003)	(0.009)	(0.021)
Panel C. Upper respiratory												
Solar_t	-0.023***	-0.024***	-0.031***	-0.017	-0.007	-0.002	-0.009**	-0.004	-0.002	-0.005	-0.002	0.001
	(0.005)	(0.005)	(0.008)	(0.016)	(0.020)	(0.032)	(0.004)	(0.006)	(0.010)	(0.003)	(0.005)	(0.008)
Panel D. Lower respiratory												
Solar_t	-0.010	0.001	0.019	-0.071**	-0.036	-0.002	-0.047**	-0.027	-0.010	-0.038**	-0.023*	-0.010
	(0.009)	(0.009)	(0.013)	(0.032)	(0.038)	(0.041)	(0.022)	(0.021)	(0.027)	(0.014)	(0.014)	(0.019)
Obs.	36,366	36,366	36,366	3,828	3,828	3,828	5,742	5,742	5,742	7,656	7,656	7,656
City fixed effects	×	×	×	×	×	×	×	×	×	×	×	×

Notes: This table displays estimation results of regressing daily hospital admissions on weekly, monthly, and yearly average solar power generation across groups of cities. Estimation results are marginal effects from ZINB regressions using 300 iterations and offsetting by population. Controls include weather, mining production, and demographic covariates. All regressions include controls, year, seasons, year × seasons, and weekend fixed effects in both the main and the inflate equations. Clustered standard errors by city appear in parentheses. Significance levels: $^{*}p < 0.10$, $^{**}p < 0.05$, $^{***}p < 0.001$.

Table A11: The Long-Term Effect of Maximum Solar Generation on the Daily Rate of Hospital Admissions

	All Cities			Cities Downwind of Displaced Fossil Fuel Plants								
				$< 10km$			$< 50km$			$< 100km$		
	t=week	t=month	t=year	t=week	t=month	t=year	t=week	t=month	t=year	t=week	t=month	t=year
Panel A. Cardiovascular												
Solar_t	-0.025***	-0.026	-0.027***	-0.064	-0.059	-0.067	-0.028	-0.025	-0.028	-0.028**	-0.026*	-0.028**
	(0.006)	(0.017)	(0.007)	(0.054)	(0.054)	(0.055)	(0.019)	(0.019)	(0.017)	(0.014)	(0.014)	(0.014)
Panel B. All respiratory												
Solar_t	-0.027***	-0.022***	-0.018**	-0.046***	-0.018*	-0.004	-0.022**	-0.008	0.001	-0.023***	-0.013	-0.005
	(0.007)	(0.006)	(0.007)	(0.014)	(0.009)	(0.025)	(0.009)	(0.010)	(0.041)	(0.005)	(0.008)	(0.012)
Panel C. Upper respiratory												
Solar_t	-0.021***	-0.021***	-0.020***	-0.014	-0.004	-0.003	-0.009**	-0.002	-0.002	-0.005	-0.001	-0.0002
	(0.005)	(0.005)	(0.006)	(0.014)	(0.018)	(0.019)	(0.003)	(0.005)	(0.006)	(0.004)	(0.005)	(0.005)
Panel D. Lower respiratory												
Solar_t	-0.004	0.002	0.007	-0.047*	-0.031	-0.013	-0.032**	-0.024	-0.014	-0.026**	-0.022*	-0.012
	(0.008)	(0.008)	(0.008)	(0.025)	(0.033)	(0.029)	(0.015)	(0.018)	(0.017)	(0.011)	(0.012)	(0.011)
Obs.	36,366	36,366	36,366	3,828	3,828	3,828	5,742	5,742	5,742	7,656	7,656	7,656
City fixed effects	×	×	×	×	×	×	×	×	×	×	×	×

Notes: This table displays estimation results of regressing daily hospital admissions on weekly, monthly, and yearly maximum solar power generation across groups of cities. Estimation results are marginal effects from ZINB regressions using 300 iterations and offsetting by population. Controls include weather, mining production, and demographic covariates. All regressions include controls, year, seasons, year × seasons, and weekend fixed effects in both the main and the inflate equations. Clustered standard errors by city appear in parentheses. Significance levels: $^{*}p < 0.10$, $^{**}p < 0.05$, $^{***}p < 0.001$.

Table A12: Descriptive Statistics on Fine Particulate Matter ($PM_{2.5}$) Concentrations

Variable	Mean	Std. Dev.	Min.	Max.	Obs.
Panel A. All Cities					
$PM_{2.5}$	14.74	6.89	3.39	47.80	5,780
Panel B. Cities $\leq$ 10km Downwind of Displaced Fossil Fuel Plants					
$PM_{2.5}$	17.49	7.51	3.58	47.80	2,784

Notes: This table displays main descriptive statistics of fine particle matter concentrations for cities with available data. Panel A corresponds to data from four cities hosting fossil-fueled power plants (Alto Hospicio, Antofagasta, Arica, and Tocopilla. Panel B corresponds to data from two cities near and downwind of displaced fossil fuel plants (Alto Hospicio and Tocopilla). Data are daily records averaged across stations from 2012 to 2017, and come from the National Air Quality Information System (SINCA)'s website https://sinca.mma.gob.cl.

Table A13: The Effect of 1 GWh of Solar Generation on the Daily Rate of Hospital Admissions Using a Poisson Estimator

	All Cities		Cities Downwind of Displaced Fossil Fuel Plants					
			$< 10km$		$< 50km$		$< 100km$	
	(1)	(2)	(1)	(2)	(1)	(2)	(1)	(2)
Panel A. Cardiovascular								
Solar_d	-0.024*	-0.022	-0.060	-0.059	-0.044	-0.040	-0.033	-0.030
	(0.014)	(0.014)	(0.070)	(0.069)	(0.044)	(0.039)	(0.032)	(0.028)
Panel B. All respiratory								
Solar_d	-0.066***	-0.067***	-0.144***	-0.144***	-0.094***	-0.093**	-0.080***	-0.078***
	(0.015)	(0.014)	(0.041)	(0.041)	(0.028)	(0.029)	(0.019)	(0.021)
Panel C. Upper respiratory								
Solar_d	-0.027**	-0.027**	-0.032***	-0.033***	-0.021***	-0.021***	-0.017***	-0.017***
	(0.008)	(0.009)	(0.007)	(0.005)	(0.005)	(0.004)	(0.003)	(0.003)
Panel D. Lower respiratory								
Solar_d	-0.013***	-0.013**	-0.127***	-0.125**	-0.084***	-0.081**	-0.070***	-0.067***
	(0.003)	(0.006)	(0.038)	(0.041)	(0.025)	(0.028)	(0.017)	(0.020)
Obs.	36,385	36,385	3,830	3,830	5,745	5,745	7,660	7,660
Number of Cities	19	19	2	2	3	3	4	4
City-fixed effects	✓		✓		✓		✓	
City × year-fixed effects		✓		✓		✓		✓

Notes: This table displays estimation results from regressions of daily hospital admissions on daily solar power generation using a Poisson estimator (offsetting by population). Solar generation is in GWh. All regressions include weather, mining production, demographic covariates, and year, seasons, year × seasons, and weekend fixed effects. Clustered standard errors by city appear in parentheses. Significance levels: $^{*}p < 0.10$, $^{**}p < 0.05$, $^{***}p < 0.001$.

Table A14: The Effect of 1 GWh of Solar Generation on the Daily Rate of Hospital Admissions Using an OLS Estimator

	All Cities		Cities Downwind of Displaced Fossil Fuel Plants					
			$< 10km$		$< 50km$		$< 100km$	
	(1)	(2)	(1)	(2)	(1)	(2)	(1)	(2)
Panel A. Cardiovascular								
Solar_d	-0.003	0.0003	-0.038	-0.039	-0.035	-0.036	-0.020	-0.017
	(0.041)	(0.041)	(0.109)	(0.110)	(0.056)	(0.057)	(0.047)	(0.044)
Panel B. All respiratory								
Solar_d	-0.115**	-0.114**	-0.324	-0.325	-0.184	-0.188	-0.253	-0.251
	(0.054)	(0.054)	(0.283)	(0.282)	(0.206)	(0.209)	(0.156)	(0.159)
Panel C. Upper respiratory								
Solar_d	-0.027	-0.027	-0.080	-0.080	-0.044	-0.046	-0.053	-0.054
	(0.020)	(0.020)	(0.063)	(0.062)	(0.046)	(0.044)	(0.032)	(0.032)
Panel D. Lower respiratory								
Solar_d	-0.085*	-0.085*	-0.263	-0.263	-0.152	-0.151	-0.193	-0.190
	(0.041)	(0.041)	(0.243)	(0.244)	(0.173)	(0.179)	(0.124)	(0.130)
Obs.	36,385	36,385	3,830	3,830	5,745	5,745	7,660	7,660
Controls	✓	✓	✓	✓	✓	✓	✓	✓
City-fixed effects	✓		✓		✓		✓	
City × year-fixed effects		✓		✓		✓		✓

Notes: This table displays estimation results of regressing daily hospital admissions per 100,000 people on daily solar power generation using an OLS estimator. Solar generation is in GWh. All regressions include weather, mining production, demographic covariates, year, seasons, year × seasons, and weekend fixed effects. Clustered standard errors by city appear in parentheses. Significance levels: $^{*}p < 0.10$, $^{**}p < 0.05$, $^{***}p < 0.001$.

Table A15: The Effect of 1 GWh of Solar Generation on the Daily Rate of Hospital Admissions Using a Negative Binomial Regression Model

	All Cities		Cities Downwind of Displaced Fossil Fuel Plants					
			$< 10km$		$< 50km$		$< 100km$	
	(1)	(2)	(1)	(2)	(1)	(2)	(1)	(2)
Panel A. Cardiovascular								
Solar_d	-0.025*	-0.022	-0.060	-0.059	-0.044	-0.040	-0.033	-0.030
	(0.014)	(0.029)	(0.071)	(0.070)	(0.044)	(0.039)	(0.033)	(0.028)
Panel B. All respiratory								
Solar_d	-0.067***	-0.068***	-0.142***	-0.142***	-0.091**	-0.090**	-0.079***	-0.077***
	(0.016)	(0.017)	(0.040)	(0.040)	(0.028)	(0.029)	(0.020)	(0.022)
Panel C. Upper respiratory								
Solar_d	-0.030**	-0.030**	-0.037***	-0.037***	-0.023***	-0.023***	-0.020***	-0.019***
	(0.009)	(0.009)	(0.007)	(0.005)	(0.005)	(0.004)	(0.003)	(0.003)
Panel D. Lower respiratory								
Solar_d	-0.038***	-0.039	-0.125***	-0.123**	-0.082***	-0.079**	-0.069***	-0.066***
	(0.009)	(0.055)	(0.037)	(0.040)	(0.025)	(0.028)	(0.017)	(0.020)
Obs.	36,385	36,385	3,830	3,830	5,745	5,745	7,660	7,660
Controls	✓	✓	✓	✓	✓	✓	✓	✓
City-fixed effects	✓		✓		✓		✓	
City × year-fixed effects		✓		✓		✓		✓

Notes: This table displays estimation results of regressing daily hospital admissions on daily solar power generation using a Negative Binomial model. Solar generation is in GWh. All regressions include weather, mining production, demographic covariates, year, seasons, year × seasons, and weekend fixed effects. Clustered standard errors by city appear in parentheses. Significance levels: $^{*}p < 0.10$, $^{**}p < 0.05$, $^{***}p < 0.001$.

Table A16: The Effect of 1 GWh of Solar Generation on Placebo Outcomes

	All Cities		Cities Downwind of Displaced Fossil Fuel Plants					
			$< 10km$		$< 50km$		$< 100km$	
	(1)	(2)	(1)	(2)	(1)	(2)	(1)	(2)
Panel A. Infections								
Solar_d	-0.010	-0.009	0.008	0.008	0.003	0.002	-0.004	0.0001
	(0.006)	(0.006)	(0.020)	(0.017)	(0.005)	(0.008)	(0.004)	(0.007)
Panel B. Blood-Related Diseases								
Solar_d	-0.00002	-0.001	0.003	0.002	0.001	-0.0001	0.001	-0.0002
	(0.001)	(0.002)	(0.017)	(0.012)	(0.005)	(0.014)	(0.004)	(0.016)
Panel C. Strokes								
Solar_d	-0.003	-0.003	-0.001***	-0.0001	-0.004	-0.004	-0.002	-0.001
	(0.010)	(0.033)	(0.0002)	(0.005)	(0.023)	(0.006)	(0.007)	(0.125)
Panel D. Bone Fractures								
Solar_d	0.000	0.000	0.017	0.020	0.005	0.009	0.005	0.001
	(0.026)	(0.131)	(0.021)	(0.020)	(0.021)	(0.026)	(0.139)	(0.048)
Panel E. Appendicitis								
Solar_d	-0.021*	-0.021**	0.023	0.025	0.031**	0.021	0.021**	0.019
	(0.011)	(0.008)	(0.028)	(0.082)	(0.013)	(0.016)	(0.008)	(0.014)
Obs.	36,385	36,385	3,830	3,830	5,745	5,745	7,660	7,660
Number of Cities	19	19	2	2	3	3	4	4
City fixed effects	×		×		×		×	
City×year fixed effects		×		×		×		×

Notes: This table displays estimation results from regressions of daily hospital admissions on daily solar power generation. Estimation results are marginal effects from ZING regressions offsetting by population. Controls include weather, mining production, and demographic covariates. All regressions include controls, year, seasons, year × seasons, and weekend fixed effects in both the main and the inflate equations. Clustered standard errors by city appear in parentheses. Significance levels: $^{*}p < 0.10$, $^{**}p < 0.05$, $^{***}p < 0.001$.